12-4-2016

Mechanical and Physical Characterization of Foams made of Gelatinized Starch and Pre-polymer Polyurethane

Baxter J. Lansing
bjl2505@rit.edu

Mechanical and Physical Characterization of Foams made of Gelatinized Starch and Pre-polymer Polyurethane

By

Baxter J. Lansing

A Thesis Submitted in Partial Fulfillment of the
Requirements for the Degree of Master of Science in
Packaging Science

College of Applied Science and Technology
Department of Packaging Science
Rochester Institute of Technology
Rochester, New York

December 04, 2016

Approved by: Professor _____ Date: _____ (Thesis Advisor)

Dr. Changfeng Ge

Professor _____Date:_____ (Committee Member)

Prof. Deanna Jacobs

Professor _____ Date: _____ (Committee Member)

Dr. Christopher Lewis

I. Acknowledgements

This study could not have been accomplished without the help and support from everyone in the packaging science department and has been an opportunity second to none. Professor Changfeng Ge it has been a pleasure to work in the American Packaging Laboratory with you on the many different research projects. I have learned so much more. Professor Deanna Jacobs I have enjoyed our many conversations and your always bright spirited nature. Professor Christopher Lewis I appreciate your guidance in my research and our many talks.

I feel fortunate to become friends with each one of you and will reflect on it for many years to come.

I would also like to say thank you to Tim Tuner and Jack Burruto for help with data collection and data verification, best of luck to you guys.

To mom, dad, my sisters, grandpa, aunts & uncles, friends and Rusty dog who have been there for me over the years and support all my crazy endeavors in which I greatly appreciate your patience and loving support.

II. Abstract

Previous work in this field of research has proven that the intrinsic properties of native starch can be modified to have desirable traits. For example there are two widely researched natural properties of native starch: physically brittle and hydrophilic. Researchers have been successful at mixing native starch with various polyols or water to yield a modified starch with viscoelastic behavior. Furthermore low miscibility of native starch with other polymers has made it the topic of polymer blend studies to help alleviate its hydrophilic nature.

For this study materials were selected based on both previous research and ability to create test samples from corn starch that behave in a viscoelastic and hydrophobic manner. Castor oil is chosen as the polyol because it is naturally abundant, hydrophobic and proven to be reactive with isocyanate. 4,4, methylene diphenyl diisoycanate is chosen on the basis of reactivity with castor oil and corn starch.

The aim of this study is develop and characterize foam materials derived from corn starch and a pre-polymer made from castor oil and 4,4, methylene diphenyl diisocyanate. Castor oil and 4,4, methylene diphenyl diisocyanate polymerize to yield random urethane crosslink's. When gelatinized starch and the pre-polymer are mixed, secondary interactions between these 2 components are evident. The effect of chemical and physical foaming agents is analyzed, where chemical foaming agents behave both exothermic and endothermic, the physical foaming agent behaved endothermic. In addition the change in starch proportion is also investigated. Results show different mechanical behavior from what is found in literature and can be attributed to direct fraction of gelatinized starch and both type and dispersion of foaming agent.

Table of Contents

III. List of Figures

IV. List of Plots

V. List of Tables

VI. Introduction

Foams are integrated into the world around us and are utilized in a wide range of anthropogenic artifacts. To be more specific; foam can be defined as a solid or liquid matter containing an internal 3 dimensional structure of cells/voids and this internal structure can contain matter in the form of gas or liquid. Common examples of liquid foam are fire retardant and laundry detergent, solid matter foam is found in furniture cushions, headphone speaker covers, and consumer product packaging. Both liquid and solid foams are made from synthetic or naturally occurring polymeric material(s). However from here on only solid foams will be discussed. The viscoelastic characteristic of solid polymer foam has resulted in many practical solutions to consumer products as noted above and even more precisely product packaging. It is evident that short cradle to grave life of consumer product packaging has led to more research and development of less inert foam material but still deliver adequate performance?

With the above question in mind many terms or phrases have been associated with short life cycle products for example; bio based, green, biodegradable, compostable, renewable, sustainable etc. These terms have been under close watch; according to Scot Chase [1] of TerraChoice in 2010 there were as many as 500 different terms found on labels of products indicating some type of environment friendly aspect of their product and this is known as greenwashing. To avoid confusion in the following study a distinction between two types of foams will be made: first are naturally occurring foams known as natural resources. The second type of foam are man-made also known as synthetic foams and because the constituents of the main product can be in very crude form and minor changes from the natural state, these materials are modified either chemically or mechanically and are thus not found naturally in that state. The second type of foam will be the topic of discussion.

Natural occurring polymeric foams such as, cork and the sea sponge are great examples of foams that have found their way into the household. The former of the two examples can also give an historical perspective to the importance of foams. It is harvested from the cork oak tree (Quercus suber L) and is native to the Mediterranean region notably Spain and Portugal. One of the first applications of cork as a modern packaging material was in Epernay, France where monk Don Pierre Perignon began to use cork as the stopper in wine bottles in 1680. Yet archeological evidence from Mediterranean sites suggest cork lids for urns maybe as old as 3000

years old [2]. The cork material is typically harvested from the outer layer of the tree known as phellogen (bark) and remarkably the tree is the only species worldwide that can survive having its entire outer bark structure removed. The cell structure of the outer bark is a closed cell and each individual cell is a polygon where the number of sides differ with respect to the direction of tree growth. From a microscopic perspective the cell wall consist of a very interesting layered composition of organic compounds (mass %): suberin (58%), lignin (12%), cellulose (22%), cerin (2%), water (5%) and other (1%) and each composition is an approximation because of varying growth rate in each tree [2]. Interestingly the natural quality of cork to be chemical resistant and gas impermeable is because of the high suberin content. Even more so when cork is subjected to compression stress the material is able to sustain a strain rate as high as 80%. A reliable figure of 374,000 tons of cork is harvested annually [3].

On the other hand synthetic polymer foams are designed into many household products such as furniture or egg cartons as well as many high volume products. Example of high volume applications for synthetic foam are coffee cups made from Styro-foam™, loose fill foam in corrugated boxes as well as foam inserts found inside corrugated packages. In each of these applications the foam material differs according to the physical structure, which is dependent upon the design intent, i.e. thermal properties, fragility or compression and rebound behavior [4]. Synthetic foams dominate nearly the entire foam market in the US where it is estimated that the demand could reach 8.6 billion pounds by year 2017. By volume the packaging industry is expected to consume 30% of the overall demand and from another perspective one-third of the overall market demand will be polystyrene due to its wide array of properties i.e. thermal insulator, light weight [5].

Polymer foams are classified into two main categories: thermosets and thermoplastics. Thermosets are polymers which commonly involve mixing 2 counterparts that chemically react to form a network microstructure. Once solidified or “cured” the material cannot be re heated to be reshaped or formed because the bonds created within the network structure are chemical bonds, also known as crosslinks which form irreversible covalent bonds [6]. One of the most widely utilized polymers for thermoset foams is polyurethane (PU) and it should be noted that PU can be polymerized into both thermoset and thermoplastic. Thermosets are typically utilized in structurally demanding applications and are not discussed within this study.

In contrast to the network structure, thermoplastics are long chains characterized by both molecular weight average (M_w) and number average molecular weight (M_n). Chain microstructure is commonly characterized as branched or linear. As mentioned above PU can also be polymerized into a thermoplastic, commonly referred to as thermoplastic urethanes (TPU)[8]. In contrast to creating crosslinks, physical bonds i.e. hydrogen bonds, are created between chains (intermolecular forces). Upon reaching a known temperature, affinity between these chains is temporarily lost allowing for transient chain movement and ultimately fluid like behavior. The nature of thermoplastic polymers allows them to be re-heated into a liquid state and then shaped multiple times. Polymers that are commonly converted into foam include polystyrene (PS), polyethylene (PE) and polypropylene (PP) [6].

Processing of thermoplastic foams is performed on 2 different magnitudes; industrial and laboratory. Typical processes used to make foam include: extrusion, injection molding, compression molding and casting [6]. These processes are traditional and widely applied to foam and non-foamed polymers at both magnitudes. Unlike the above examples a truly unique process was developed for expanded polystyrene (EPS) and should be reviewed because of its extensive use in packaging. In the 1^{st} step pellets are put into a chamber where both heat in the form of steam and pentane gas are introduced and cause the pellets to expand nearly 40 times the original size where each pellet develops a closed cell network. The pellets are then moved to a separate chamber to dimensionally stabilize for a specific time duration. Last, pellets are conveyed into a heated mold where both steam and vacuum cause the pellets to form into the shape of the mold [7].

The cellular network inside the foam can be one of two structures: open cell and closed cell. Open cell foams are typically permeable to gases and liquids in addition to having poor thermal conductivity. Closed cell foams have very low permeation rate and low thermal conductivity. Chemical foaming agents such as alkali carbonate, sodium bicarbonate and sodium borohydride are typically used to extrude closed cell foams. Introduced into the melt as a fine powder or granule, through thermal decomposition or chemical reaction the powder changes state into a gas, causing cells to initiate throughout the melt matrix. Open cell foams are typically manufactured with physical foaming agents like CO_2, nitrogen and even liquids such as water. Introduction of physical foaming agents into the extruder usually occurs in the metering section before the die. At elevated temperatures liquid evaporates into a gas and because of low melt

viscosity cell growth creates a tortuous structure inside the polymer melt. In special cases both physical and chemical foaming agents have been used together [9].

Foams found in the packaging field meet a diverse array of design requirements such as thermal conductivity, energy absorption, liquid absorption and even anti-static properties. Cold chain distribution requires low thermal conductivity to minimize temperature fluctuation during shipping where typical products inside could be foods or medical supplies. Thermal conductivity can be described as the flow rate of heat through an object. The following are examples coefficients for relevant solids; PU=0.030 W/m^{o}C, EPS=0.046 W/m^{o}C. and, Glass 0.78 W/m^{o}C [10]. Conductivity changes with temperature such that a lower temperature is directly related to lower conductivity.

Energy absorption is a very common application for foams in packaging and two different methods are used to understand how foam materials can absorb a mechanical force. The first method of measuring energy absorption is the compression test. Below in figure. 1 is an ideal compression curve for expanded polystyrene (EPS) where a sample was compressed in a cyclic method. When the sample is placed between two platens and force is applied two different curves can be measured; the upper curve is the foam being compressed and the bottom curve is the reaction force of the foam as the platen is traveling in the reverse direction (the form is pushing back on the platen). The change between the upper and lower curves can be quantitively characterized as hysteresis; how much energy the foam absorbs during the initial compression. If a cyclic compression method is carried out as in figure 1 multiple upper and lower curves are generated and the change in slope is due to the viscoelastic nature of polymer foams. However complete recovery from deformation is possible.

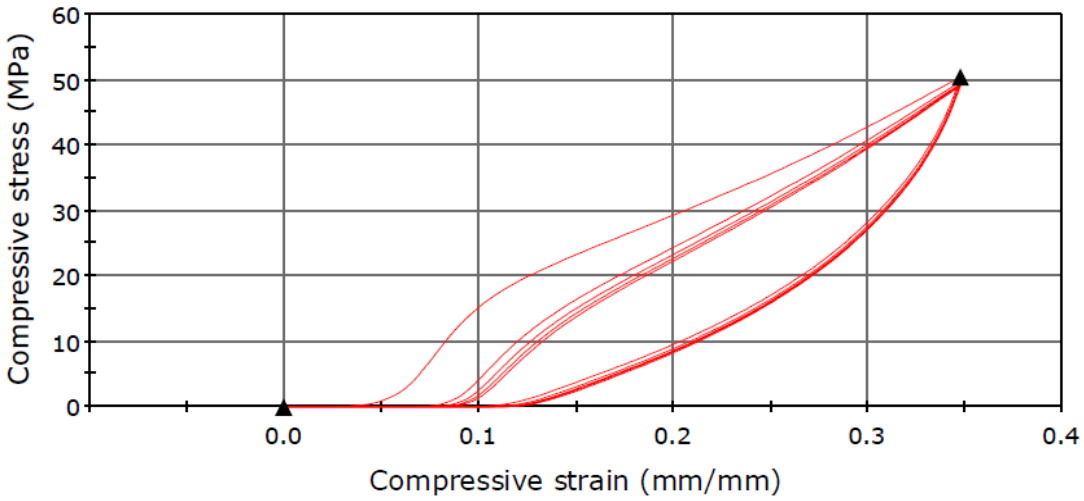

Figure 1- EPS Compression at 50% Strain

The second method is known as cushion testing where cushion curves are generated. These curves are specific to testing packaging foam for the ability reduce or avoid product damage. A general description of the test is as follows: a sample of simple geometry is placed atop a stationary platen. Above the sample is a guided platen in which mass is added or removed. The sample then remains static and the guide platen is raised to a predetermined height and released into a free fall and impacts the foam. Combinations of added mass and varying height are measured for samples of the same geometry.

A plot as seen in figure 2 is constructed. In an ideal scenario the foam sample will dampen impact which is evident by a parabolic curve. The most practical information that can be extracted from the graph is where the foam can keep the product from being damaged. From left to right the plot is initially a negative slope followed by a region of zero slope and finally a transition into positive slope. The static stress found in the middle region of zero slope can be used to determine the foam sample surface area needed to avoid product damage of a specific mass and drop height. At zero slope the foam has completely absorbed impact energy from the fall and the transition to a positive slope indicates the foam has experienced permanent deformation thus exceed energy absorption capacity [11].

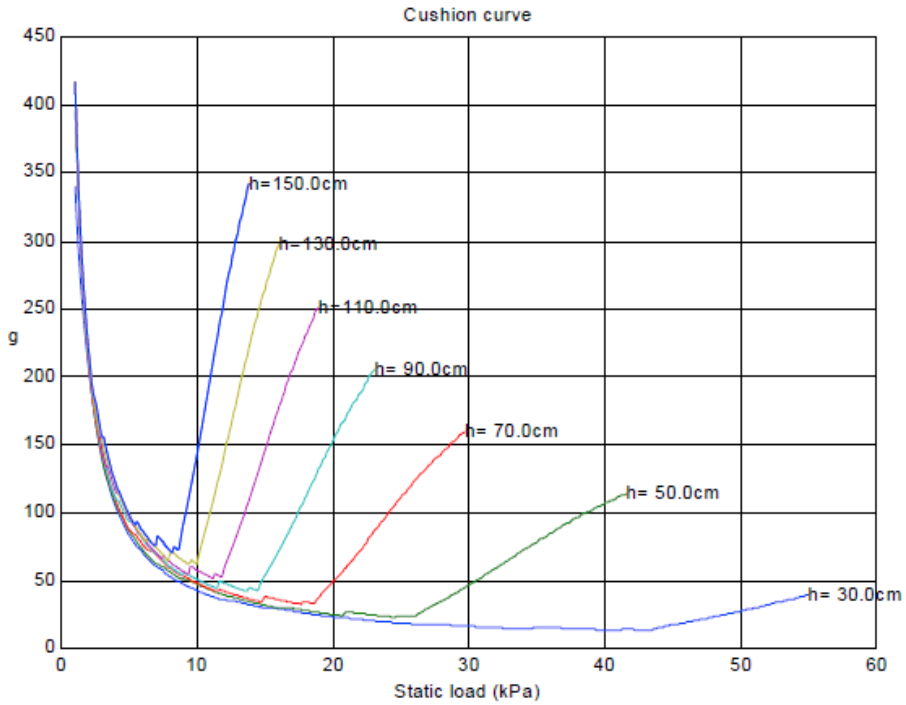

Figure 2-Example dynamic Cushion Curves from BASF

The two other design requirements that were mentioned, liquid absorption and anti-static, will be discussed briefly due to their relevance. Liquid absorption of foam changes with both type of material, olefins such as polyethylene (PE), polypropylene(PP), or polystyrene(PS) are not greatly affected by water absorption where as foam made from starch can become weak, if not disintegrate when subjected to high humidity. Simultaneously mechanical properties will also diminish. This behavior is called hydrophilic in contrast to foams that do not absorb moisture are termed hydrophobic. Secondly, electrostatic discharge (ESD) or electro conductive foams are specialty materials that are utilized in very special circumstances because of their high cost. Currently there are two types of ESD foams which involve a conductive material and matrix material: carbon filler based and doped. Carbon based foams are simple and require traditional equipment. Doping polymers requires equipment with high temperature capability in addition to a halogen such as Br_2. Overall ESD foams are used to dissipate static charge to avoid having a short in micro circuits and thus reduce faulty products.

Concluding remarks are on different foams which are available in today's market among which have already been discussed. Currently there are foams made from the byproducts of harvesting natural resources such Evocative © foams derived from solid biomass waste and mycelium. The biomass is described as agricultural waste but not specifically identified [12].

The internal cell structure is anisotropic, where mycelium creates flexible domains and the agriculture waste is rigid. Another type of foam is manufactured by Green Cell Foam™ from KTM industries, which is entirely made from non-genetically modified corn starch. Together these companies are primarily targeting the distribution and shipping markets with more sustainable packaging solutions [13]. The types of materials mentioned above can be distinguished as being derived from renewable resources in contrast to non-renewable which are resources that cannot be replenished in anywhere near the same time as renewable resources but can be recyclable [14, 15]. Furthermore it should be noted that these two different types of resources are described for the purpose of research and to avoid green washing.

Previous work in this field of research has proven that the intrinsic properties of native starch can be modified to have desirable traits. For example there are two widely researched natural properties of native starch: physically brittle and hydrophilic. Researchers have been successful at mixing native starch with various polyols or water to yield a modified starch with viscoelastic behavior. Furthermore low miscibility of native starch with other polymers has made it the topic of polymer blend studies to help alleviate its hydrophilic nature.

One area of research that is successful at modifying the intrinsic properties of native starch is deriving a blend of polyurethane and native starch. Polyurethanes are commonly made by reacting isocyanate (-N-C-O-) with a monomer or low M_w fluid (< 5000 g/mol) containing hydroxyl groups (-OH-), i.e. starch, polyethylene glycol, glycerol and castor oil. The product of the reaction is a macro molecule containing urethane linkage as seen in figure 3.

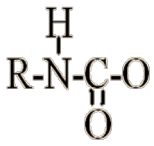

Figure 3-Urethane repeat unit

For this study materials were selected based on both previous research and ability to create test samples from corn starch that behave in a viscoelastic and hydrophobic manner. Castor oil is chosen as the polyol because it is naturally abundant, hydrophobic and proven to be reactive with isocyanate. 4,4, methylene diphenyl diisoycanate is chosen on the basis of reactivity with castor oil and corn starch. The physical function of each component in the blend

is castor oil will be the soft segment, corn starch is the hard segment and 4,4, methylene diphenyl diisoycanate will create miscibility between the former two components.

The aim of this study is develop and characterize foam materials derived from corn starch and a pre-polymer made from castor oil and 4,4, methylene diphenyl diisocyanate. Castor oil and 4,4, methylene diphenyl diisocyanate polymerize to yield random urethane crosslink's. When gelatinized starch and the pre-polymer are mixed, secondary interactions between these two components are evident. The effect of chemical and physical foaming agents is analyzed, where chemical foaming agents behave both exothermic and endothermic, the physical foaming agent behaved endothermic. In addition the change in starch proportion is also investigated. Results show different mechanical behavior from what is found in literature and can be attributed to direct fraction of gelatinized starch and both type and dispersion of foaming agent.

VII. Literature review

Polymer foams have been derived from renewable and non-renewable resources. The focus of the literature review will be on foam or polymer alike derived entirely or partly from similar materials as used in the proceeding study. Articles that are discussed will be in context to the introduction and perhaps with more emphasis on materials, methods, and results. Historically, researchers began to study synthesis of these foams in the early half of the 20th century and commercialized in the second half [16].

1. Foaming agents

A reprint from the encyclopedia of polymer science and technology of the late 1950's gives a great understanding of the science behind blowing/foaming agents [17]. They particularly focus on physical foaming agents because at the time industry heavily used and understood these materials. Jumping ahead the immediate differences in chemical and physical foaming agents are how they thermodynamically behave. Physical foaming agents are liquids that have a wide range of boiling points that are similar to a polymer melt temperature. Through vaporization of the physical foaming agent the melted polymer matrix forms a cellular structure and once rapidly cooled the structure is retained. Physical foaming agents change their state of matter but do not necessarily change their chemical structure, usually in an endothermic fashion. These should also be non-harmful to humans and non-damaging to processing equipment, i.e.

corrosive. Chemical foaming agents on the other hand thermally decay and products of their decomposition form gases which expand to create a cellular structure. This process of decomposition is typically irreversible and exothermic but not strictly so (e.g. bicarbonates). Physical and chemical foaming agents can be mixed to achieve different foaming results, but neither one should act as a solute or solvent in regards to the polymer matrix.

An endothermic chemical foaming agent Sodium bicarbonate is and has been one of the most widely used foaming agents in recent times. Typically around 120-267mL of gas per gram of Sodium bicarbonate is yielded in the following reaction:

$$2\ NaHCO_3(_s) \rightarrow Na_2CO_{3\ (S)} + CO_{2\ (g)} + H_2O\ (_g)$$

Alongside sodium bicarbonate, stearic acid can be incorporated as an activator to help increase gas yields. It is estimated that in the reaction above there should be twice as much CO_2 gas available with addition of stearic acid. Critic acid can also be incorporated for the same purpose as stearic acid of to increase decomposition temperature of the foaming agents. Another foaming agent of important commercial success is benzenesulfonyl hydrazide (BSH). At thermal decomposition 115-130 mL/g of nitrogen are produced and 195mL/g of steam (per gram of BSH). Further chemical tailoring of the BSH structure can create a substantially higher decomposition temperature. Typical decomposition of an asymmetrical BSH molecule is seen below.

$$NH_2NH - SO_2 - C_6H_6\ (_s) \rightarrow S\text{-}C_6H_6\text{-}S\ (_s) + N_{2\ (g)} + H_2O\ (_g)$$

Dr. Mergenhagen [18] has been working in the foaming agent industry for some time and his proceedings after the conference were published giving an introduction to chemical foaming agents. In regards to the previous article from the early 1950's Dr. Mergenhagan considers Sodium Bicarbonate and critic acid to be economically the most important endothermic chemical foaming agent. Furthermore the European Union (EU) only allows endothermic chemical foaming agents for food contact applications. Exothermic chemical foaming agents he notes are auto-catalytic because once the reaction begins temperature increase from decomposition increases the rate of the reaction, BSH is an example of these types of foaming agents.

A 5 step process on chemical foaming process for thermoplastics is discussed, where 1st the polymer and foaming agent are mixed, 2nd the polymer melt and foaming agent interfaces are evening distributed, 3rd nucleation site form, high pressure will increase the sites at which cells will form, 4th is where the polymer –gas byproduct moves into the nucleation sites and cell growth is apparent. And last the polymer melt is cooled and cell growth is stabilized.

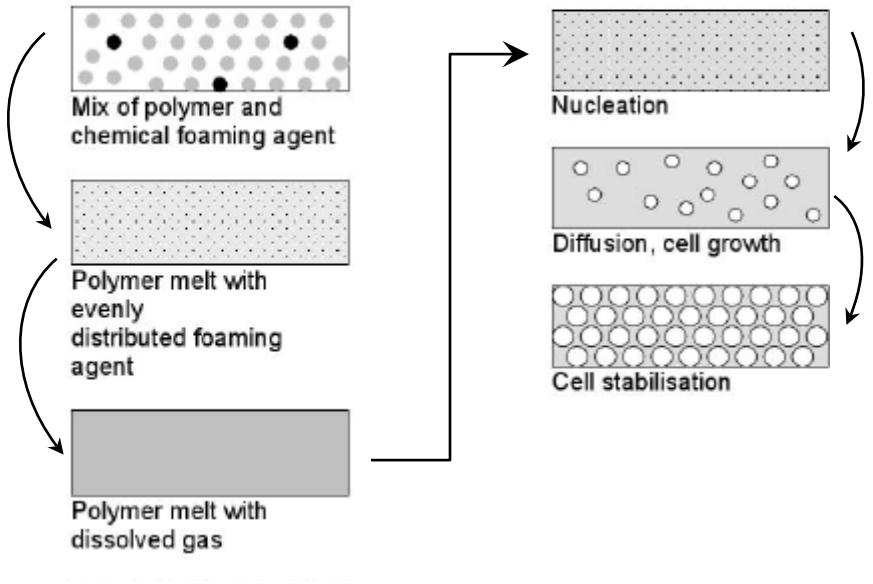

Figure 4-Foam agent mechanism

Stabilization of the cells is important; if the cell walls become too thin they can coalescence. If viscosity is too high then cell size will decrease. For physical foaming agents the process is similar minus the first step. Addition of the foaming agent into the processing machine often requires special equipment. For thermosets the foaming process consist mainly of two steps. First, the foaming agent and polymer are mixed below the decomposition temperature. Then the crosslinking agent is mixed in and the whole batch is mixed to the curing temperature. Unlike thermoplastic foaming agents which are in liquid or powdered form. Thermoset foaming agents are mostly in particle form with no nucleation step.

2. Materials

4, 4’ Diphenyl methane Diisocyanate (MDI) according to Wittcoff, H. A., Reuben, B. G., & Plotkin, J. S. [19], is the most important raw material in polyurethane production. In 2008 98,000 tons of MDI were produced in the United States of America alone. It is made through a 2 step reaction. First Aniline hydrochloride and formaldehyde are reacted to form 4, 4’ Diaminodiphenylmethane. Treatment with Phosgene yields MDI. The entire reaction is seen below in Fig 3.

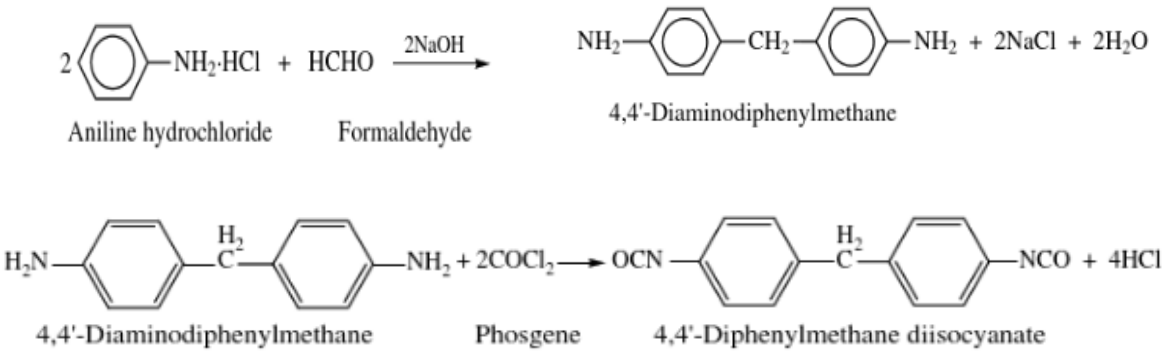

Figure 5-MDI synthesis

Unfortunately phosgene is a very toxic substance and alternate methods of making MDI are being researched but no methods have been commercialized. In 2008 53% of USA MDI production went to the rigid foams market. Another 9% went to flexible foam market.

A review [20] on the castor oil plant (Ricinus communis) brings to light various aspects on agriculture/horticulture, economic importance, industrial application and safety concerns. Castor oil is extracted from the seed of castor bean plants. Typical processes include solvent extraction, hot pressing and cold pressing, where combinations of the three methods can also be applied. Further refinement of the oil is done chemically remove phospholipids and heavy metals when water and acid are introduced. Second, a physical absorption process is carried out to remove pigments, traces of soap and odor causing compounds. The remaining biomass of the castor bean such as the husk are unsafe to both human and animal. It is mentioned that 4 castor beans are toxic to a 160lb human. Toxicity of the residual waste is from high ricin and ricinine content, one of nature’s most poisonous substances. Remaining biomass can be detoxified through steam, boiling, autoclaving and heat treatment. When put into solution with NaOH,

NaCI and tannic acid to name a few, detoxification also takes place. It should be noted that harvesting of castor beans for their oil exposes workers to these toxins.

Thailand, Brazil, China and India are four major exporters of castor oil. In 2007 India alone exported over 800,000 tonnes of castor oil or 70% of the market share. The largest importers of oil are USA, Russia, and Japan. These countries find use for castor oil as medicine, pre-cursor and monomer of many. Furthermore, sources suggest that castor oil has been in use since ancient Egypt and the Persian Empire. Specific modern industrial applications include BASF's polyamide (PA) 6, 10 where sebacic acid is derived from castor oil or 100% castor oil based PA 11. Dehydrated castor oil is found in varnishes, resin systems and adhesives. Wide array of applications has caused high demand for castor oil and need for acceptable substitutes and genetically modified plants with less side effects from toxic side effects. Genetic engineering and traditional cross pollination have created plants with 99.9% reduction in ricin content. Plants such as the Wrightia tinctoria and Lesquerella fendleri are being analyzed for comparison to ricinoleic acid, the key molecule found in castor.

In regards to use for PU materials the authors' devote an entire section. Castor oil is able to be blended with various polyols to achieve ductile behavior i.e. 410% at break where an isocyanate is typically incorporated as a crosslinking agent. One of the major governing parameters is the stoichiometric ratio of NCO/OH groups. A ratio of 1 yields a ductile product where as a ratio of 2 yields a more brittle product. Of more importance is their discussion of interpenetrating polymer networks also known as blended polymers. In agreement with the above statement when the NCO/OH ratio increases for a castor oil/ PET blend elongation decreases and tensile strength increases. Another interesting project found that polymerization of polyacrylonitrile (PAN) and castor oil resulted in creation of a porous hydrogel structure with a 50 fold improvement in mechanical properties of PAN [20].

A second review on castor oil written by [21] points out more details on castor oil. Each castor bean contains approximately 46-55% CO. As noted above it is grown in tropical and sub-tropical climates. One of the major aspects of CO is the fact that it is not edible or readily used in the preparation of human foods and conflict between managing feedstock for food or industrial processes favors the latter. In addition to the above applications CO is specifically used as a lubricant for high performance auto-mobile and jet engines.

Starch is a complex natural resource which has found itself as a topic in many different fields. As stable carbohydrate in many diets, food scientist Wang, S. and Copeland, L. [22] provide great insight into the molecular disassembly of starch. Divided into 4 subtopics; Introduction on importance of starch, 2nd; the granular structure of starch, 3rd gelatinization of starch and 4th retrogradation of starch. A more scientific name of starch is polysaccharide as seen in its natural state. However most starches whether for food or material use are hydrothermally treated. In general hydrothermal treatment involves a fluid, heat, and pressure or shear forces. The change in macromolecule structure that occurs during and after hydrothermal treatment has been under investigation since the early 70's.

There are two theoretical models for the structure of a starch granule as seen below in figure 6 the size of starch granules varies with the type of starch i.e. corn, potato, etc. and ranges in size from 1- 100 µm. It is agreed on that there is alternating patterns of amylose (linear) and amylopectin (branched) regions. Crystalline regions form lamella. Furthermore each section of the pattern contains both amylose and amylopectin structures. However each section is mainly composed of one type of structure. Granule b is structure that resembles growth rings in a tree trunk. Structure C is a relatively new type of structure analogous to a spider web. Both models agree that amylose is centered and is known as a hilum.

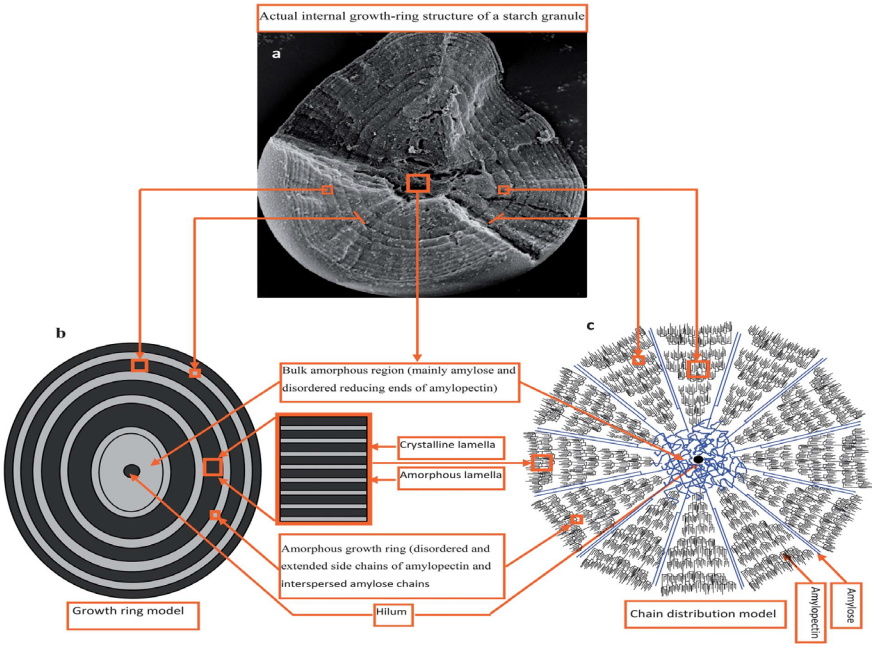

Figure 6-Starch granule microstructure (Photo courtesy of Wang, S. and Copeland, L)

Gelatinization of starch in research literature often involves reaction with polyols; however these authors simply discuss gelatinization of starch in water. The word gelatinization implies that the initial structure seen above has been disrupted and irreversibly altered. It is thought that amylose chains absorb moisture initially and swell creating pressure, causing amylopectin chains to slowly unfold. Once chains unfold evidence suggest that inter molecular forces form single and double helixes. Overall gelatinization requires proper amounts of water and heat 65-96.7% and 50-80^{o}C respectively. These percentages are not absolute and depend upon the type of plant that starch is harvested from.

Finally retrogradation of starch occurs after starch has been gelatinized and cooled down, often in storage. Visually it is notice by change in gel viscosity, opacity and phase separation. Retrogradation is effectively changing from a complete random structure to a discernible structure hence the change in opacity. Amylose chains retrograde hours after gelatinization, whereas amylopectin can take days; both are temperature dependent. If gelatinization involves a polyol a network like structure of single helix amylose may form. In absence of a polyol a aggregated mass may form.

Zia, F. et. al. [23] published a review on starch and urethane blends where sample preparation of film was common but foam samples are discussed. Literature finds starch to be a high molecular weight polymer: amylose typically has a M_w of 1 – 1.5 x10^6(g/mol) and amylopectin has M_w of 50 – 500 x 10^6(g/mol). Amylose is considered to be a branching unit and thus an amorphous bulk structure where as amylopectin is considered to be a linear crystalline in structure. They further define the plasticization and gelatinization of starch with regards to the two structures above. Where starch is inherently a brittle substance with the addition of water or polyol the amylopectin become de-structured and once this occurs thermoplastic or gelatinized starch is formed. The European Union paper and corrugated industries have the largest market share at 30% in native starch. Niche applications include food, sanitary products, and lubricant thickener these current applications making it hard to justify immediate new uses of starch.

One finding that appears to be consistent among published research is the stoichiometric ratio between NCO/OH groups is usually 2.0 or less. In a blend of starch and PU mechanical properties reciprocate approximately at 20% starch however additional materials or processes can be implemented to achieve an interpenetrating polymer network (IPN) for optimum material properties. One such way is to react starch and another organic substance such as: vinyl-

trimethoxysilane, glycerol, water or even acetylation. A second method is to create a graft polymer of starch and another polymer. The copolymer is then reacted with isocyanate. They found great reduction in moisture absorption. Further techniques to creating a more optimal blend of starch and PU is to add nano-composites and nano-fillers. One of the more promising nano-fillers in starch and PU blends are starch nano crystals. An investigation on synergistic behavior between water borne PU and starch nano crystals and additional cellulose whiskers at 0.4 w/w% found an increased in tensile strength of up to 252% for water borne polyurethane. Strong hydrogen interacts at the interface were detected. Another investigation on incorporating only starch nano-crystals found massive increases in tensile strength and modulus (6720%) suggesting the samples were quite rigid.

A second review of castor oil brings to light important details on the wide applications of castor oil based polyurethane and concerns of material safety. Shirke, A., Dholakiya, B.[24] and Kuperkar, K. write that castor oil has good shelf life with the exception when exposed to high heat. The reaction between castor oil and various isocyanates occurs in the range of 60-75^{o}C and is considered to be exothermic. Further contents of the review include Hybrid materials, interpenetrating polymer networks, foams, coatings and adhesives.

They classify foams into 3 groups; flexible, semi-flexible and rigid and castor oil based PU can be made into any of the 3 groups. Other researchers have produced flame retardant foam where the addition of castor oil increased thermal stability and compression strength. Others found that semi-flexible foam is possible when reacting only castor oil and isocyanate. In other applications castor oil PU has been successfully applied to anti-corrosion coating and super adhesive for other polymers and metals. They also mention that a stoichiometric ratio greater than 2 is very harmful and could cause acute poisoning.

3. Early work of Polyurethane and Starch

In 1957 Dosman & Steel [25] filed for a patent titled “Flexible shocking-absorbing polyurethane foam containing starch and method of preparing same”. Their invention is described as 2 basic components; organic polyisocyanate and poly-functional or polyester material and in contrast to other synthetic foams they incorporated corn starch into the PU matrix. Their new foams are described as spongy, flexible and an increased modulus per unit density, in other words the foam is able to withstand more stress at similar densities. Method of

foam preparation is most simplistic: a pre-polymer is created by making an aqueous solution of the two basic components mention above in the absence of water vapor. Second, water and starch are mixed into a second homogenous emulsion. Additional constituents which tailor the foam to specific requirements include: urea for urethane for linkages and catalyst. The catalyst is added when in contrast to a polyol, a polyester is reacted with the polyisocyanate. Furthermore polyethers and polyamides are other substitutes. A specific ratio of reactive hydrogen atoms in the prepolymer is stated as 1.0-1.25 (isocyanate/ polyester or the like). The ratio for mixing the aqueous solution to the homogenous emulsion varies from 0-100 parts where the sum of each part is equal 100. Once the reaction has initiated CO_2 gas is a byproduct of the reaction and thus a cellular network is formed.

Following the work of the two previous authors another research team was able to develop rigid polyurethane foam by incorporating a chain extender additive and ultimately various flame retardant compositions (Bennett, Otey, & Mehltretter [26]. Their study utilized polymethylene polyphenylisocyanate (PAPI) and Tetrakis (2-hydroxypropyl) ethylenediamine (Quadrol) in the prepolymer. Corn starch and dextrin, a modified type of starch, were added into the solution. Furthermore a foaming agent known as trichlorofluromethane was also added, however the boiling point is near room temperature making preparation more tedious. Starch preparation was unique in comparison to other researchers in that these authors used a hammer mill to pulverize starch and then further size exclude via different sieves. Nearly 60% of the starch passed through a #230 sieve. To differentiate between blends they developed a characterization method based on the ratio of isocyanate groups (NCO) to hydroxyl groups (OH) ranging from 62 to 113. Their experiment achieved foam with 10, 20, 30 and 40 (%w/w) starch. Following the change in ratio, the study examined viscosity, density, compression strength, flammability, water absorption, fungi resistance and closed cell composition. For each increase in starch content compressive strength decreases by a factor of 0.7. Other significant findings include reduced flammability with increase loading and overall starch PU foam yielded favorable results over dextrin in all areas besides fungi resistance.

Two years later another article was published from Otey and colleagues [27] on PU derived from diphenylmethane diisocyanate (MDI), castor oil reacted with glycol glycosides and milled corn starch. Glycol glycoside is formed from alcoholysis of castor oil and glycol (polyol). The reaction of these 3 materials took place inside a 250 cc flask under vacuum and nitrogen

atmosphere. It should be mentioned that neither temperature nor viscosity are mentioned when these 3 materials are mixed together. It is mentioned that an exothermic reaction should initiate before pouring contents into a mold. The concentrations of each material varied and the effect on physical properties was quantified using a 2^{nd} degree multiple regression. Variables of the regression include starch concentration (0-60%Wt), molar ratio of isocyanate groups to hydroxyl groups (1.0, 1.1, 1.5 and 2.0) and last the polyol content by equivalent hydroxyl weight.

They find a correlation between high polyol concentration and increased sample strength as a result of crosslinking where as lower concentrations of polyol result in a high probability of crosslinks between isocyanate groups, polyol and starch but show minimal increase in strength. On the other hand in figure 3 starch concentration appears to have a major influence on elongations of the blends. A polyurethane sample with 60% starch did not exceed 10% elongation regardless of the NCO/OH ratio. With 0% starch, elongation measured was between 50% and 97%, in addition to these results their regression had an 85.9 % correlation. Tensile strength had 89.5% correlation, flexural strength 75.2% correlation, defection had an 83.5 correlation and shore D hardness had the highest correlation of 91.0%. In conclusion the authors suggest that a NCO/OH ratio should be greater than 1.5 to achieve desirable properties at relatively low cost.

In 1972 Otey and co-workers [28] publish another article on the reactivity of modified starch and isocyanate that yielded 14 polymers with characteristics of both thermoset and a thermoplastic. Their experiment involved various forms ester starch, a catalyst triethylenediamine and toluene diisocyanate or phenyl isocyanate, at this state it is intuitively a pre-polymer. Castor oil was then added to a stoichiometric ratio of NCO to OH equaled 2 and the viscous mixture was poured into a mold heated at 140^{o}C for 15min under 500 p.s.i. The amount of starch added was 20% equivalent weight to the resin mixture. Results from the experiment contrast the fact that native starch is only soluble in water or dimethylsulfoxide (DMSO), however the derived polymers are insoluble in water, acetone, ethyl ether, or ethanol. And yet more interesting, four of the polymers show melting behavior in the range from 178^{o}C to 248^{o}C whereas others only softened or showed no changes. In regards to tensile results polymers that show inert thermal characteristics achieved tensile stress of 3100 p.s.i whereas polymers with appreciable thermal behavior yielded have a tensile stress of up to 7100 p.s.i. They suggest the change in tensile stress is caused from a decrease chain length of C_{18} to C_8. Overall their

concluding remarks make clear that these results are not optimum, but are informative preliminary findings.

Integrating starch into polymers on the commercial scale was envisioned quite some time ago by Otey [29]. As a contributing author in the above articles, Otey presented a review on the current and potential commercial uses of starch and polymers. In section II 3 major polyols are discussed in the manufacture of PU foams containing starch; sorbitol, methyl glucoside and glycol glycosides. Where sorbitol was currently being used in commercial PU, methyl glucoside had some commercial scale success and glycol glycosides had been evaluated at the pilot scale and found to be feasible. However the author identifies the reason for limited or no commercial success of the above polyols to be rapid fluctuations in market prices; $0.185/lb to $0.420 in a duration of 3 years. In the long run they were unable to remain cost competitive. Furthermore it is noted that the market price of starch had only fluctuated $0.04 per lb in the past 2 decades. Pilot studies on commercial scale plants from 7 different companies yield feasible results however in addition to unstable prices of the polymer constituents the end product, PU was determined to have an unstable demand, making any product unworthy of investment.

In section III Otey describes the use of starch as filler in plastics, and mentions a major demand for disposable packages in municipal and alike applications can be expected. Matrix plastics discussed are polyethylene (PE) and polyvinyl chloride (PVC). Studies on these blended plastics and their biodegradable behavior were measured through mold propagation. Further on, starch as a reactive filler with isocyanates is discussed in short detail. Isocyanate is blended with another liquid containing hydroxyl groups. At this step a pre-polymer has been created and isocyanate should be in excess to allow for further bonding with starch. Finally starch is added to the mixture ranging from 10% to 60% by mass. The addition of starch was reported to increase solvent resistance, decrease chemical costs and chemical bonds were formed between the pre-polymer and starch.

4. Fillers

Chen, Y., Zhang, L., Deng, R., and Liang, H. [30] prepared 12 different blends of soy dreg, castor oil (CO) and toluene diisoycanate (TDI). Each component differed in weight content and the ratio between NCO groups to OH groups (TDI to CO). Ratio of soy dreg incorporated was 50%, 60%, and 70% and the TDI and CO masses were based off the ratios 2.00, 1.67 and

1.33. The scope of the study was to compatibilize castor oil with soy dreg using toluene isocyanate. After preconditioning the materials a single screw extruder was used to melt blend each combination and in sequence were molded for 7 min then fan cooled. Using Attenuated Total Reflection (ATR) technique spectrum were collected and observations of isocyanate groups and hydroxyl groups are discussed. Their first observation indicates that there were no unreacted -NCO- groups because of an absence of a peak at 2272 cm^{-1}. Evidence that the TDI is compatiblizing CO and SD was determined when a peak at 1651 cm^{-1} became broader and more intense peaks were measured at 1724-1732 cm^{-1} indicating the increase of carbonyl groups (-C=O). Stronger evidence is observed at 3374 cm^{-1} which are characteristic of –N-H, -O-H and –N-H_2 segments. These segments can be attributed to castor oil or soy dreg molecules.

Differential scanning calorimetry (DSC) results further support the ATR findings. The glass temperature ranged from -24 to 22^{o}C and can be interpreted through the amount of soy dreg and molar ratio of isocyanate to castor oil. Soy dreg is composed of soy protein and cellulose segments that have no quantitative glass transition (T_g) temperature from their DSC method. However sample blends show a measureable T_g such that as soy dreg proportion increased the glass transition temperature increases for samples with a molar ratio of 2 Tg is equal to22^{o}C. Samples with a molar ratio of 1 exhibit maximum a T_g equal to -24^{o}C at 50 %w/w soy dreg. As the TDI proportion increases interaction with CO and soy dreg also increase causing Tg to shift to more positive values at 50 (%w/w) soy dreg. In contrast to TDI proportion as soy dreg proportion increases to 60 and 70 (%w/w) the Tg incrementally decreases. Thus maximum interactions are observed at 50 (%w/w) soy dreg.

Jute fiber, derived from plant species Corchorus capsularis & C. olitorius [31] was an interesting component in a polymer matrix [32]. Commonly observed in burlap bags, jute fiber is a relic of bulk packaging. Their sample films were prepped 2 different ways; first, castor oil, maleic anhydride (3:1 molarity), Tung oil 20(%w/w), initiator(20%w/w), jute fiber 60 (%w/w) and catalyst cobalt naphthenate (20%w/w). The second method decreased weight proportions of castor oil, initiator (2%w/w) and jute fiber 60 (%w/w) along with a catalyst cobalt naphthenate (2%w/w). The second method did not incorporate Tung oil. Each sample was compression molded at 130^{o}C. Relevant results include thermodynamic behavior of the reaction, FTIR spectra and contrasting mechanical properties. Using the DSC they found the curing temperature to occur between 130-160^{o}C without adding jute fiber. When more catalyst was added curing

temperature reduced to 40-125 ^{o}C. For both scenarios an exothermic peak was observed around 220^{o}C and was attributed to maleic anhydride modified castor oil molecules forming intermolecular bonds. Both FTIR and ^{1}H NMR results did not investigate this scenario. However FTIR spectroscopy was able to determine that a reaction occurred. At 3450 cm^{-1} a peak for -OH- absorption was found in neat castor oil, after the reaction this peak decreased and a peak at 1640 cm^{-1} increased indicating the formation of –C=C bonds in the modified castor oil. No peaks at 1779cm^{-1} and 1849 cm^{-1} were detected which is an indication that nearly all the maleic anhydride molecules had reacted. The addition of maleic anhydride caused the polymer to behave more ridged. Impact resistance increased 42% compared to unmodified castor oil samples. In contrast the strain at break increased by a factor of 2 for unmodified castor oil samples.

Found in the paper and pulp industry as a byproduct, cellulose was further refined to a nano-scale filler [33]. Starch based foams were then prepared with nano fibrillated cellulose (CNF) into a starch water matrix. CNF is just one unit the makes up a complete cellulose molecule which is perhaps one of the world's most abundant macromolecules. CNF can be derived chemically or mechanically. The content of both starch and CNF remained in single digit percentages. The CNF, starch and water suspension is put into a high shear mixer for 20mm at 1700 RPM. Samples are poured into trays and freeze dried for 250min. Sample characterization methods consist of SEM images, density and relative density, porosity, volume fractions, flexural testing, TGA, thermal conductivity and compression testing.

As solids content increases density, compression strength and modulus of elasticity increase proportionately. Flexural strength vs. density was plotted to find a curvilinear plot. On the other hand porosity increased with less solid content and is thought to be the result of CNF interacting with starch. Authors note that compression results to be similar with Styrofoam™ packaging and packaging foam in general. Thermal conductivity was also examined for insulation applications.

As previously mentioned cross link density is one factor that can control how rigid a PU foam will behave. Another method is discussed by [34] where they modified castor oil to increase -OH- concentration and added pine wood fiber for rigidity. The hydroxyl count of modified CO is 449 mg KOH/g versus 392 KOH/g for a commercial polyol. The ratio of NCO/OH groups ranged from 1.00 to 1.25. The foaming agent used was a hydrochloroflurocarbon at 10 (%w/w). Polyol, surfactant and catalyst are mixed inside a reactor

and then last MDI is introduced. Sample formation is simple: the mixture is poured into a cup to cure under ambient conditions with no post curing operation. Among data collection compression and density are of most interest. However the physical- chemical techniques used find the wood flour to be a reactive filler with the PU matrix, they add wood flour in at 0% 10% and 15% (%w/w).

For the commercial polyol derived PU, addition of 15% wood flour caused density to decrease from 37 kg/m^3 to 36 kg/m^3. However contrasting results are found with PU derived from modified castor oil. With the addition of 15% wood flour density increased from 37.0 kg/m^3 to 38.0 kg/m^3. Even more interesting, the less dense commercial polyol derived PU yields higher compression modulus and yields stress, 4.2MPa and 146.0 kPa for 15% wood flour addition as compared to modified castor derived PU with 15% wood flour (2.1 MPa and 116.8 kPa respectively). An explanation with respect to PU without wood flour is deduced from cell structure observations: when wood flour is introduced into the mixture MDI interacts with both the polyol and wood flour causing cell walls to be more fragile due to decrease in cell size and poor dispersion. Micro-cracks are also initiated at the interface of wood flour and PU.

5. Water born polyurethane (WPU)

Water born polyurethane (WPU) is achieved when the reaction to create polyurethane takes place within a water medium. Furthermore water is reactive and is the final step of the polyurethane polymerization. Gao, Z., et. al.[35] produce WPU films from castor oil, polyethylene glycol (PEG), and isophorone diisocyanate and cellulose nanocrystals derived from eucalyptus lignin. Samples were simply prepared by pouring the emulsion into a petri dish and placed under vacuum and dried for 1 week with cellulose concentrations of 0, 0.2, 0.5,1,2,3,4 and 5 (%w/w).

Their films were characterized via FTIR, atomic microscopy, TGA, DSC, and tensile testing. For tensile testing five samples were tested at strain rate of 100 mm/min in ambient conditions. The effect of adding cellulose crystals can be considered a two way interaction. From 0%-1% tensile strength at break increases by a factor of two, the change in elongation is negligible and the only significant change in modulus is from 0% to 0.2%. When cellulose levels reach above 1.0% the effects are reversed: elongation and rupture stress decrease significantly

and modulus increases. Their explanation for tensile behavior is supported via FTIR when blends contain 0% - 1.0%, the cellulose creates hydrogen bonds with the polyurethane interface. Beyond these concentrations the cellulose self-agglomerates.

Water borne polyurethanes made from starch plasticized with glycerol, castor oil and isophorone diisocyanate (IPDI) are examine by French researchers Lu, Y., Tighzert, L., Dole, P. and Erre, D.[36]. Sample preparation consists of mixing castor oil and IPDI inside a 4 necked flask under nitrogen atmosphere for 4 hours at 95^{o}C. The polymer was then cooled to 40^{o}C and diluted with acetone to reduce viscosity and mixed with distilled water to create waterborne PU. Starch preparation included plasticizing starch (70%w/w) with glycerol (30%w/w) and water (10%w/w) at 140^{o}C. The mixture was feed into a single screw extruder set to approximately 120^{o}C processing temperature and 40 RPM to create thermoplastic starch (TPS). The last step was mixing TPS and waterborne PU inside the same extruder and machine parameters. PU content were as follows; 0, 4, 10, 15, 20, 30 (%w/w) in TPS.

Sample characterization includes FT-IR, DSC, DMA, morphology, tensile strength, water contact angle and water absorption. DSC and DMA examined the blends for miscibility. A single glass transition is observed in blends with less than 20% PU suggesting that there are secondary interactions between the two materials. Contradicting results are found with DMA, the mechanical loss factor (Tan δ) reveals different peaks which are associated with two phase system. In agreement with DSC results, elongation at break and tensile strength show an increasing trend (176% and 5.1 MPa) to 15% PU content and a decline after 15% PU. Measuring the area under the curve the authors are able to determine toughness of the material. 10% PU blend was able to sub stain up to 8.8 MPa making it the toughest sample. It should be noted that the units for toughness are incorrect; toughness should be reported in Joules.

6. Blends and Interpenetrating networks

Kumar and Kaur [37] developed rigid urethane foams based off of MDI, castor oil with 10% glycerol and cobalt octoate catalyst. A physical foaming agent (n-pentane) was used. Their materials were first mixed inside a 4 necked flask and nitrogen atmosphere. MDI to castor oil ratios were 1:1, 2:1 and 3:1. An increase in MDI was reported to create a more rigid sample. Foam samples were created by pouring the mixture into a closed mold for duration of 24hrs.

Their samples were characterized through tensile, compression, water absorption test and morphology.

Interestingly, tensile results increased with addition of MDI and compression values show marginal increase. A suggestion is made that high NCO/OH ratio creates lower molecular weight chains and lesser degree of crosslinking. Furthermore, in the discussion on compression results they suggest that load bearing capacity increases with NCO/OH ratio. Under the discussion on morphology, a general observation is made in that both cell size and density decrease with the increase in NCO/OH ratio. Water absorption results show that the lowest NCO/ OH ratio (1:1) absorbed the most water with a 38.99% increase over initial mass. Water absorption for samples made with a NCO/OH ratio of three absorbed the least amount (22.75%).

A copolymer of castor oil, maleic anhydride and diluent styrene monomer is made into foam by Wang, J, H. et.al. [38] where their characterization consists of GPC, H^1NMR, FTIR, density, compression, SEM and soil degradation tests. Foamed samples were made first by reacting Maleic anhydride and castor oil inside a 250mL 4 necked flask. After a range of 0.5 to 9 hours styrene monomer was added and mixed for only seven minutes. Viscosity increases when 4 phr of water is added. Foaming agent $NaHCO_3$ (sodium bicarbonate) at 1.5 to 3.75 phr was also mixed in. Density was inversely affected by foaming agent concentration; at 1.5 phr concentration density measured was 0.35 g/cm^3 and at 3.75 phr density measured 0.12 g/cm^3.

Their compression data was collected at 2 mm/min and 10% strain. Five samples were tested with the mean and standard deviation reported. Two general conclusions can be observed. With the addition of styrene monomer increases modulus and compression strength also increase. However as styrene monomer content decreases density appears to increase along with sample flexibility. Furthermore they attribute differences in compression values to both cell size and curing time. In other words smaller cells resulted from curing at 65^{o}C which produced smaller cells and lower compression stress. And vice versa for foams cured in ambient conditions. To determine which factor; styrene concentration or density was more influential on mechanical properties a power-law regression was used. As a result the inherent properties of the styrene monomer are more influential.

The miscibility of starch and castor oil blends is studied by Cao, X, Wang, Y. and Zhang, Y.[39]. Their blends incorporate 4, 4'-diphenymethane diisocyanate (MDI), modified corn starch and castor oil. The modification of starch was chemically intensive due to the reactions

that took place at 3 different stages. First starch and sodium chloride and sodium hydroxide were reacted to obtain ethyl starch (ES). A second starch labeled benzyl starch (BS) was also produced. The second stage is creating a pre-polymer by mixing MDI and castor oil. And finally, pre-polymer and modified starches are mixed and poured onto a glass plate and formed into a film where modified starch concentrations were 10, 20, 30 and 40 (%w/w).

Miscibility of the samples was analyzed through FTIR, elemental analysis, GPC, intrinsic viscosity, DSC, DMA, optical transmittance and tensile properties. The authors find all pre-polymer-starch blends miscible besides ES-40. In each of the different characterization techniques results indicate that phase mixing and secondary interactions are far greater for BS blends than ES blends. Such that water absorption maximum for ES film is 12% whereas BS films absorb a maximum of 3.2%. A similar situation is observed with elongation: maximum elongation for ES films is 16% whereas BS reached elongation of 157%.

One of the most influential research publications in this review is the work performed by Wu, Q. et. al. [40] on starch and polyurethane. The aim of their study is to create a tough starch which is also thermoplastic. Materials consist of 4, 4' MDI, corn starch and castor oil. A pre-polymer of castor oil and MDI was created inside a 500 mL 3 necked flask under 2 mmHg. A stoichiometric ratio of two isocyanate groups to one hydroxyl group was maintained. Modified starch was created simply by placing starch powder, water, and pre-polymer into the intensive mixer at 95^{o}C 100 RPM for 25 minutes. Sample preparation was simply done by placing the modified starch into a compression molder to create a film for five minutes at 100^{o}C.

Samples were analyzed for moisture absorption, tensile properties, FTIR, DMA, viscosity, SEM WAX and TGA. A clever technique is used to determine how much isocyanate has reacted. Authors submerged samples into toluene to remove any unreacted urethane groups. The difference in initial and final mass was put into proportion to find how much isocyanate reacted to form urethane links. Authors' observation of SEM pictures show micro phase separation and unequal dispersion of pre-polymer/polyurethane. Further examination of miscibility is demonstrated by placing a sample in toluene a second time for 24hrs. Toluene is known to cause polyurethane to swell [41], hence disrupting the micro-phase. More SEM images show little to no disruption of the micro phase after the second trial of submerging indicating miscibility. Furthermore solubility of starch is tested when samples are submerged into water.

SEM images appear to show little or no deterioration of the micro phase. In both scenarios it is believed that urethane linkages are foamed between castor oil and starch via MDI.

Tensile data shows similar trends for both elongation and stress at break. Native starch is interpreted as brittle and urethane is interpreted as ductile. They compare plain modified corn starch with starch and PU blends. Where elongation increased more than a factor of 2 due to urethane linkages formed between starch and polyurethane increased elongation. A final comment from the authors' are that samples are able to undergo secondary processing, in other words thermoplastic behavior was observed.

Starch in modified formation was examined by Skočilas, J., Žitný, R and Šesták, J. (2010) [42]. Their study seeks thermodynamic constraints behind closed mold foaming of potato starch. Material description is vague, however they begin with a potato starch that has been gelatinized with water. The gelatinized starch is then placed into a heated rectangular mold. Mold temperature ranged from 120 – 140^{o}C. The mold is fitted with five thermal couples and one pressure transducer to study the effects of starch foam expansion. Their results reveal a direct relation between sample thickness and peak mold pressure. For instance, for a maximum expansion height of 2 mm maximum pressure is found at roughly 20sec. When sample height increases by a factor of 2 the time also increases by a factor of 2. Furthermore they examine porosity of each sample and find their maximum porosity occurs simultaneously as maximum pressure. A final observation finds little variance in porosity longitudinal but changes in the transversal direction.

Tan, L., Su, Q., Zhang, S. and Huang H.[43] utilized a commercially available thermoplastic polyurethane to blend with TPS and compatibilizer. Utechllan UE-95A TPU (extrusion grade), TPS, polyolefin elastomer (POE) and Nitrile butadiene rubber (NBR) were blended together at different ratios using a twin screw extruder. Samples were made into sheets with a compression molder as well as injection molded tensile and impact samples. Characterization of samples was carried out through FT-IR, DSC, SEM, tensile, impact and folding endurance, DMA, surface energy and water absorption with deionized water.

FT-IR results indicate that NBR reduces miscibility between TPU and TPS however POE works well as a compatibilizer due to the a decrease of –NH- and -OH- groups and an increase in inter and intramolecular hydrogen bonds. Blending TPU and TPS together without POE is also successful. At 1702 cm^{-1} peak intensity is greater for TPU/20TPS (%w/w) than for neat TPU,

indicating hydrogen bonds. SEM images show mixing techniques worked thoroughly. Dispersion of each constituent in the blend is continuous and free of cracks. DSC also shows signs of miscibility between the TPU and TPS. Change in the glass transition temperature (T_g) is observed where neat TPU is -33.6^{o}C and neat TPS is 82.2 ^{o}C. As the blend ratio changes towards a more even proportion T_g moves closer to the median value. The addition NBR caused the materials to remain immiscible.

In regards to sample vigor all three mechanical test (tensile, impact and folding endurance) give evidence of this. For example specimens made of 80TPU/20TPS/10 POE (%w/w), have almost identical mechanical properties as neat TPU. Neat thermoplastic starch was not tested, however the samples prepared with plain corn starch were made and exhibit significantly lower mechanical properties. Furthermore evidence of secondary interactions is observed with water absorption percentages. First, with the addition of TPS, -OH- groups found in starch and glycerol increase the water uptake by factor of 20X over neat TPU. The addition of POE absorption decreases by a factor of 12. In other words there are less polar –OH- groups in TPS.

Valero, F, M. et. al.[44] reacted yucca starch with polyethylene glycol and catalyst sulfuric acid. The reaction is known as a glycosylation reaction, where a hydroxyl group is replaced with different molecule. The same process was carried out with yucca starch and glycerol. Over 2 types of modified starch were created; polyethylene glycoside (PEG) and polyol-glycerol glycoside (PGG) respectively. Castor oil (CO) is then reacted with PEG and PGG via transesterification to increase the hydroxyl from initial count of 160mg KOH/g to 186 mg KOH/g and 223 mg KOH/g, unmodified castor oil is also used. Isophorone diisocyanate (IPDI) is then mixed with the above three variations of castor oil. Finally the modified starch, castor oil and IPDI are poured into a 1L flask and mixed together. NCO/OH molar ratio is 0.7 and 0.9. Samples were made into sheets by placing the mixture into a hermetic mold at 90^{o}C for 12 hours. Sample analysis includes physical, mechanical, solvent, and physical-chemical techniques. Physical and mechanical techniques are of most interest here.

All samples had a specific gravity of 1.00 or greater, where the lowest specific gravity is associated to the lowest loading of polyol at 5% of PEG. In regards to tensile performance increasing PEG or PGG content also increased tensile strength and modulus, hence elongation decreased proportionally. Unmodified CO yielded the greatest elongation of 250% where as 10%

PEG and PGG saw 200% and 50% respectively. Based on their physical-chemical evidence they believe that PGG to have the highest hydroxyl value leading to the greatest crosslink density and thus the most rigid structure as observed in a stress vs. strain plot where yielding stress is 25 MPa. In agreement with mechanical properties are solvent tests high crosslinking led to lower swelling capacity in CCI_4, toluene, and gasoline.

Three different blends are created by Xiong, Z. and associates [45] that contain poly lactic acid (PLA), corn starch, castor oil, and diphenylmethane diisocyanate (HDI). To help understand how each of the blend constituents can affect macro scale properties the three blends consist of: PLA/starch, PLA/CO/starch and PLA/CO/HDI grafted to starch. Grafting the HDI to starch takes place inside a 3 necked flask with a solution of 200mL of toluene, 100g of starch and non-specified amount of HDI at 60^oC for 5 hours and continuously mixing. The new grafted polymer is washed with acetone. Samples for characterization are simply melt blended inside a twin screw extruder pelletized and "oar shape" tests bars are created inside a lab scale injection molder.

Analyses of SEM images reveal poor adhesion between PLA/starch blends because voids are seen between both interfaces. Furthermore when castor oil is introduced the same voids between starch and PLA are noticed. However when HDI-g-starch is added into the blend the interface between starch and PLA appears to have fewer voids between starch granules. They also note finer dispersion of castor oil within the PLA matrix. Tensile and impact results seem to be analogous to SEM images. Where tensile and impact properties were decreased in PLA/starch blends. Addition of CO created comparable decreases in mechanical properties. On the other hand addition of HDI-g-starch increased impact strength from 18 kJ/m^2 for neat PLA to 41 kJ/m^2. Both modulus and tensile properties significantly decreased, but elongation at break increased from 5% to 68% for HDI-g-starch blends! They proposed 2 causes for aforementioned behavior either the HDI is behaving as a compatibilizer or essentially creating a 2 phase network between PLA and HDI-g-starch/CO.

Polyurethane foams are even being sought after for biomedical applications, Wang, C. et. al. [46] evaluated PU foams made from CO, polyethylene glycol (PEG) and MDI with 50/50 2,4, and 4,4, isomers. Foaming agents incorporated were dichloromethane Cl_2CH_2 and distilled water H_2O, MD, PEG and castor oil were mixed inside a 250mL reaction vessel for 3 hours at 70^oC. According to the author CO is the cross linking agent, PEG soft segment and MDI rigid segment.

The molar ratio of NCO/OH ranged from 2.78 to 1.36. Separately other materials were mixed together; silicone oil, (surfactant) triethylene diamine, (catalyst) stannous octoate (catalyst), Cl_2CH_2 and H_2O (foaming agents). Both mixtures were then mixed together, poured into a mold and allowed to free rise in ambient conditions.

By simply changing castor oil percentage from 40-60w% extensive changes in properties were yielded in compression and tensile. By increasing CO weight 20% both compression strength increased by a factor of more than 2, at rough 60% strain. Furthermore, compression resilience is 99%. Density increases with further addition of CO, where at 40% CO ρ =102.2 kg/m^3 and at 60% ρ=219.74 kg/m^3.

The effect of castor oil on foam stability and properties when transitioning from polypropylene glycol (PPG) is analyzed by Sharma, F. et. al. [47]. Their foam materials include PPG, 4,4, diphenyl methane diisocyanate (MDI), CO, bis(2-methylaminoethyl)ether, diethanol amine and a mixture of triethylene diamine and dipropylene glycol and distilled water as foaming agent. Mixing took place inside a paper cup in ambient conditions. Compression samples were made by pouring the mixture into a closed mold for 5 min.

According to SEM images the cell structure is open and packaging density of the cells increases with CO percentages. CO has a lower viscosity and more plentiful than the foaming agent thus, CO allows the foaming agent to volumetrically expand before the polymerization has finished. Ultimately they also associate bubble coalescence and rupture on the CO viscosity in addition to a decrease in cell count. Their load bearing capacity analysis is brief but indicates a 39% reduction in load bearing capacity for any sample subjected to an indentation force at their specific magnitude. Overall one of the biggest changes in samples is the change in NCO/OH ratio. Due to hydroxyl count increase with the increase in C.O. gelling strength is lost and so is foaming stability. In other words increasing CO also increases more un-bonded molecule ends.

Polyurethane foam is prepared and mechanically characterized by Kim, D. et. al. [48]. The foams were formed from the reaction of 2, 4, toluene diisocyanate (TDI) corn starch, polyethylene glycol, glycerol and foaming agent. Stoichiometric ratios of NCO/OH are 1.1, 0.9, 0.7& 0.5. Starch content also varied from 30, 40 and 50 (%w/w), making a total of 12 different samples. Three samples did not foam due to collapse of the foam. They attribute low NCO/OH ratio and low starch content for loss of the cellular structure during molding. Their reaction is accidently labeled to be addition polymerization but actually is a condensation reaction because

first it is exothermic and second CO_2 gas is a byproduct as well as a foaming agent. Densities ranges from 0.35-0.65 g/cm^3 where both increasing starch content and NCO/OH ratios correlate to higher densities. A unique pattern occurs for the 50% starch samples where samples with a NCO/ON ratio of 0.7 and 0.9 show a decreasing density compared to the two other ratios and is attributed to mold shrinkage.

Impact resistance of samples show the same trends as density, with increasing starch content impact energy also increases. Increasing the NCO/OH ratio also increases impact resistance but to less extent. They simply label the starch as a hard segment. Compression test almost follow the same trend as impact and density results. From a sample stress vs. strain plot samples with 50% starch appear to be rigid PU foam, failing at 6% strain and permeant deformation at 2.5% strain and 225 kPa. Lowering to 40% starch strain of 18.27% was achieved the molar ratio is attributed to differences in compression stresses.

7. Mechanical Analysis

Characterization of foam that is directed towards its application is most practical, Goods, H. S., Neuschwanger, L. C., Henderson, C. and Skala, M. D [49]. developed a new foam system to replace toluene diisocyanate (TDI) which is known to be carcinogenic. Their new system will replace TDI with methylene diisocyanate (MDI). The reasoning for the switch to MDI is that it has a lower vapor pressure by a 1000 fold lower than TDI it making safer to handle and work with although it is also known to be carcinogenic. Furthermore their foam application was directly targeted towards the encapsulation of electronic components in a weapon system application. Mechanical analysis includes tensile, compression and impact properties. Their new foam system is called CRETE and it is a five component system based off commercially available materials. Voranol 490 is a polyether polyol, DC193 silicone glycol copolymer surfactant, Polycat 17 tertiary amine catalyst, distilled water in different percentages as a chemical blowing agent, and Isonate 143L a modified form of MDI. Materials were mixed at 1500 rpm for 60 seconds and poured into cylindrical molds. Post curing took place inside an oven at 66^{o}C for 8 hours. Only core samples were used for data collection.

Compression results show a linear relationship between density increase and energy density (J/cm^3) increase. Furthermore a comparison of tensile, compression and impact test results demonstrate how behavior differs between each test. Tensile plots appear to endure less than half the strain that samples in compression can endure, due to failure. The major limiting

factor between compression and impact test is the magnitude of stress. Samples are subjected to much higher levels of stress in the impact test and ultimately reveal intrinsic compression behavior. In figure 14 of their report a comparison of all 3 testing techniques is shown. Typical stress in compression ranges from 1 MPa to 16 MPa & dependent on density. Whereas impact test ranges from 2 MPa to 22 MPa. Failure threshold in impact tests were considered at 60% of peak load. When looking at figure 13 60% of peak loading occurs at the intersection of compression and impact plots. Another difference between compression and impact tests is their relationship with density. As mentioned earlier compression exhibits a positive linear relationship with density where impact tests show an optimal foam density that will absorb the highest energy. Any more increase in foam density and energy absorption decreases, per figure 15. Their discussion ends on finding the theoretical modulus for closed and open cell foams dependent on Euler buckling formulations.

Research published from Ge & Huang [50] on packaging cushion performance of corner versus flat foam brings about the application based information on foams. Their sample tests included static compression testing, dynamic shock tests and digital image correlation (DIC). The most relevant information is the analysis of static compression data. Data from static compression data is used to develop theoretical compression curves that are typically derived from cushion or shock testers specifically designed for foam packaging. Starting with static compression tests the following values are recorded: Maximum compression stress (σ_m), hysteresis (energy absorption), and sample dimensions (L x W x D). The following equation was derived in their work to determine deceleration value (G):

Equation 3-Theoretical deceleration $$G = \frac{\sigma_m}{E} + \frac{H}{T}$$

Variable H is the height from which the sample will be theoretically dropped from in a cushion test and T is the sample thickness from static compression testing. Energy density (E) is found first by integrating the loading and unloading curves of a stress versus strain plot. The differences between both products is known as energy absorption. Variable E is found by dividing energy absorption by sample volume. Variable G is found for multiple compression strains until a complete compression curve can be plotted.

Samples used in their experiment are low density polyethylene (LDPE) foam made via extrusion. Their results conclude that corner foam pieces absorb more energy than flat foam

pieces and at lower strain rates there is about a 23% difference in material stress were higher strain rates can create as much as 30% difference in material stress. The difference in flat and corner foam stress is import for design because product damage is possible if the protective packaging inadequate. Over designing protective packaging would be using more materials than what is required thus wasting packing materials.

VIII. Materials and Method

Preparation of foam specimens was performed using a three step process. The order of preparation is as follows: gelatinize corn starch, second create a polyurethane pre-polymer and mix gelatinized starch with pre-polymer and foaming agent. And third allow materials to cure inside a radiant heat oven. For each of the 15 foam samples a strict process for preparation was followed to help alleviate any affects from sample preparation. All materials used to make foam were of analytical grade.

8. Gelatinization of corn starch

Gelatinizing was performed using corn starch from MP chemical (CAT# 902956) where the composition is approximately 75% amylose and 25% amylopectin. It can be visually characterized as a fine white powder. Beforehand starch powder is placed inside a radiant oven and dried for at least 24 hours at 85°C. The second component to gelatinizing corn starch is distilled water. Distilled water is prepared in house using a Pure-Hit Still model “Basic/PH4”. The condensate is estimated to have a pH range of 5.5-6.0. 150 mL of distilled water is added to a 250 mL glass beaker and heated to 81°C. Once heated, 36g of starch is added to the beaker. The mixture is agitated with an overhead Talboys model # 409 mixer at a constant temperature and RPM of 450. A pivoting blade impeller is used. After 1.5 hours of mixing the mixture has a gelatin like consistency, the gelatinized starch is sealed and stored at 11.2°C and 48% R.H. until further use. As discussed in the literature review the prepared starch retrodegraded based on visual inspection. As a result gelatinized starch was stored in the above conditions for 24 hours before use. Also it should be noted that the above process caused growth of mold on one sample, which then was not used for sample preparation. Below in figure 7 [51] are the corn starch molecule structures, the end hydroxyl groups are responsible for hydrophilic behavior. The abundance of hydroxyl groups contributes to gelatinization phenomena.

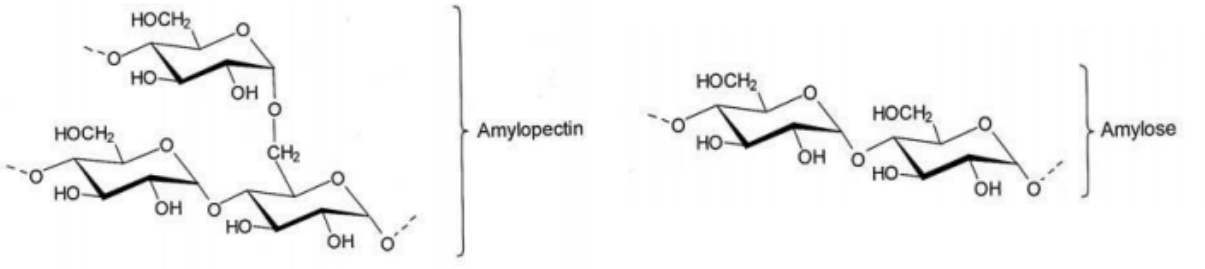

Figure 7-Corn starch molecule(s)

9. Pre-polymer synthesis

Creating the pre-polymer was a much more detailed process with greater attention needed in apparatus setup and reaction atmosphere. The process combines 2 materials to create a pre-polymer of polyurethane; Castor oil and 4, 4' methylene diphenyl-diisocyanate (MDI). As seen below in Figure 8 is the repeat unit for MDI. -N=C=O- functional groups are known as isocyanate. Urethane linkages are foamed when the double bonds are replaced by single bonds and 2 new bonds are formed at each middle carbon atom. Where as the phenyl groups find new confirmations. MDI was purchased from Acros organics with formula weight (F_w) of 250.26 and melting point of 41-44^{o}C.

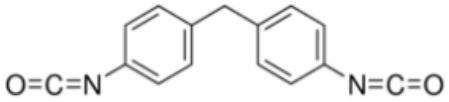

Figure 8-MDI monomer

Castor oil was purchased from Alfa Aesar with a density of 0.95 g/cm^3 and F_w of 298.46 g/mol. Castor oil is triglyceride as shown below in Figure 9. Approximately 87.7 to 90.4% of castor oil is made up of these molecules. The remaining ~10% is low molecular weight fatty acids [52]. Furthermore as a raw material the molecular composition is very consistent regardless of the region of growth. The three hydroxyl groups found and are able to react with isocyanate or MDI in this case.

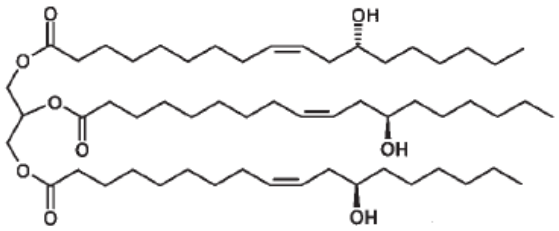

Figure 9-Castor Oil molecule.

Figure 9 is an image of the actual setup used to synthesize the pre-polymer of castor oil and MDI and Table 1 below provides the name of each component. All fittings and joints had vacuum grease applied. The procedure is as follows: 81g of castor oil is poured into the flask. To remove any residual moisture in the castor oil it was stirred for 70min at 90^{o}C , under 2.5“Hg and 350 rpm. Under vacuum and nitrogen atmosphere the flask was allowed to cool down to 40^{o}C. In the meantime MDI was pulverized from flakes into a fine powder using a mortar and pestle. Using a funnel the 61g of MDI was added to the castor oil and mixed for 40mins and reheated to 46^{o}C before mixing was completely stopped. A molar ratio of isocyanate groups to hydroxyl groups in castor oil is 2:1 respectively for all samples. The remaining isocyanate groups are anticipated to react with hydroxyl groups in gelatinized corn starch.

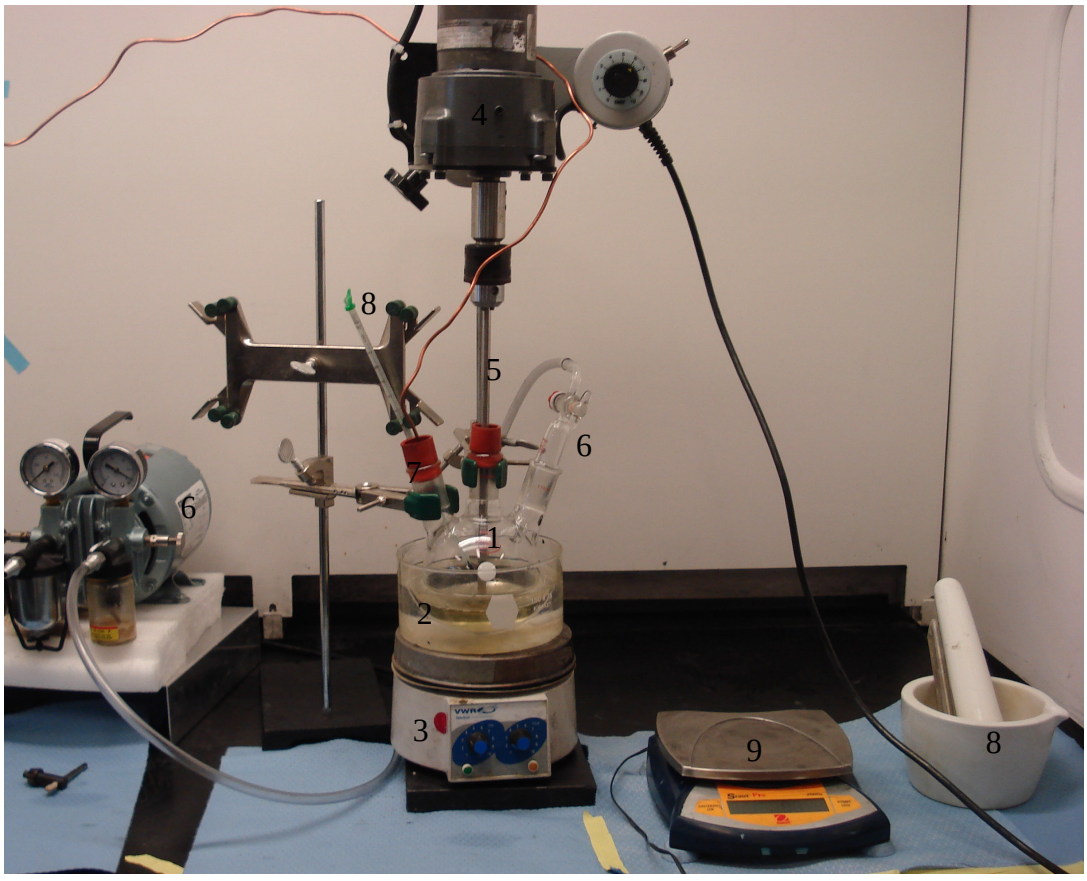

Figure 10-Actual setup for synthesis of pre-polymer

Component Number	Component
1	250mL 3 Necked Flask
2	150 x 75 Crystallization dish with mineral oil bath
3	Henery Troemner Dyla Dual Hot plate stirrer
4	Talboys 409 mechanical mixer 50-500 RPM
5	Pivoting blade impeller
6	Marathon Electric Vacuum MOD # 5KH33DN16X
6	Wilmad 90^{o} Bend Glass with PTFE Stopcock
7	Pure compressed nitrogen gas
8	Mortar pastel
9	Ohaus Scout Pro 200g scale

Table 1-Pre-polymer synthesis equipment

10. Blending Materials

Foams are typically made two different ways: continuous or batch. Continuous processes involve common equipment i.e. extruders. Batch processes involve mixing/blending materials in a pot to cure. For this work a batch process is followed. The appropriate amount of gelatinized starch is added to a Waring LB10 variable speed blender, due to retrogradation the gelatinized starch changed from a paste to a gelatin like material. The pre-polymer is added into the blender and both components are blended for 5 min while foaming agents are added, foaming agents were pre-weighted on a Ohaus Scout Pro analytical scale to 1% of the total weight of pre-polymer and gelatinized starch blend. It is observed that the viscosity greatly increases during this process. RPM is unknown however the variable speed knob is ¾ of blender's capacity. The blend is then poured into 150 x 15 culture disks and place inside a Thelco-Precision Scientific radiant oven. Oven residence time was kept to 1 hr with a target temperature of 140°C. After 1 hr the oven was shut down and allowed to cool to 55 ± 3 °C before samples were removed from the oven and stored in ambient conditions. Figure 11 shows samples with 10(%w/w) gelatinized starch and

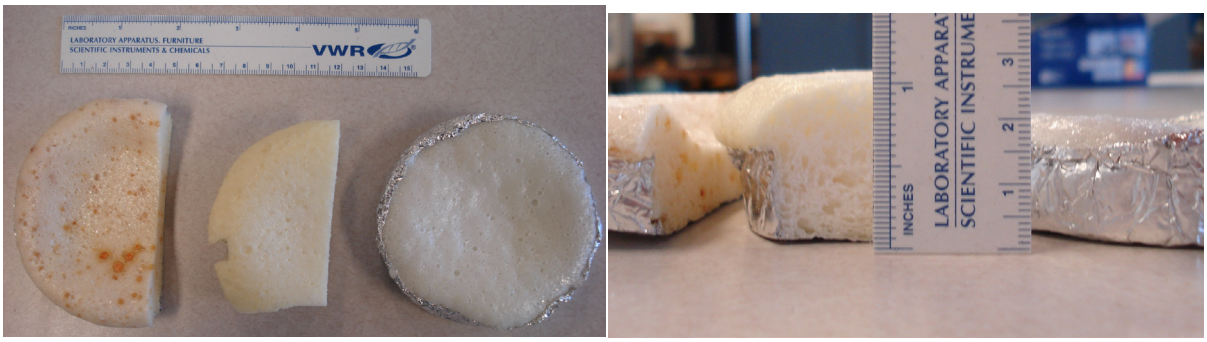

Figure 11- foam samples names left to right EXOCHEM10, ENDOCHEM10 and ENDOPHY10 respectively

different foaming agents. Each petri dish was pre-lined with tin foil for ease of sample removal and reuse. The left and middle samples have had squares removed for testing but originally were circular.

11. Foaming Agents

Foaming agents are characterized into 2 different categories: thermal degradation and change in chemical structure. Two chemical agents and one physical foaming agent were incorporated into the foam. The physical foaming agent used was distilled water than had been used to gelatinize corn starch. Water is characterized as endothermic due to heat absorption and eventual water molecules volatizing into gases. The 2 different chemical foaming agents display both endothermic and exothermic behavior. Benzenesulfonyl hydrazide (BSH) is an exothermic foaming agent that thermally degrades into nitrogen gas (N_2). BSH was in the form of a powder. It was purchased from Sigma Aldrich with an F_w of 172.2 g/mol and density of 1.36 g/cm^3. The second chemical foaming agent is comprised of 3 different constituents' sodium bicarbonate, Citric acid, and stearic acid. Stearic acid is a lubricant when the former are used in extrusion equipment. Sodium bicarbonate and Critic acid are endothermic and break down into gases CO_2 and H_2O. Both constituents are introduced in powder form. Sodium bicarbonate used was purchased from BHD with a F_w of 84.01g/mol and melting point of 50° C and is in powder form. Citric acid was purchased from EMD with an F_w of 210.14 g/mol and melting point of 135°C, in the form of a powder.

Figure 12- overlays all 3 different foaming agents and thermal degradation behavior. The oven temperature of 140^{o}C was based off of thermogravimetric analysis (TGA) seen in figure 12. TGA method is as follows: heating at 25^{o}C/min to 140^{o}C. Then an isotherm for 60 minutes. Nitrogen flow rate was set to 30 mL/min. Sample masses were 11.2 ± 0.2 mg. Afterwards the pan is cleaned by heating the oven to 950^{o}C. During the isotherm all materials exhibit thermal decomposition. Stearic acid is negligible. The addition of stearic acid is very common with sodium bicarbonate; its role is to act as a surfactant. Interestingly the chemical endothermic foaming agents are most stable at 140^{o}C. BSH and distilled water almost completely degrade. Distilled water appears to immediately thermally degrade after heating initiates. Most likely the high flow rate of purge gas causes water to evaporate.

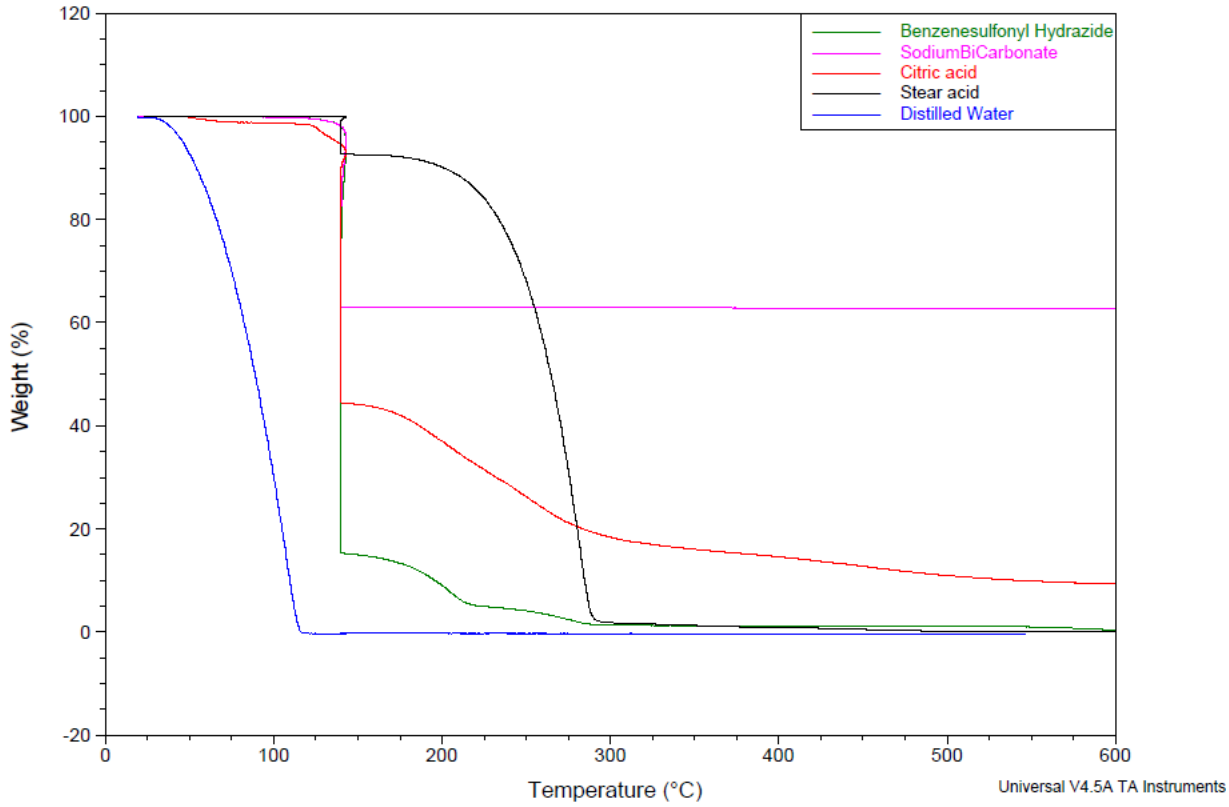

Figure 12-Thermogravimetric analysis of foaming agents

Table #2 below lists all foams made and specific name for each combination of materials. For pre-polymer constituents, castor oil and MDI amounts did not vary. The amount of starch was increased to produce a different blend. Foaming agent concentration remained at 1% for both Sodium Bicarbonate/Citric acid and BSH. Sample nomenclature is found in the last column, where ENDO is abbreviated for endothermic, EXO is exothermic, CHEM is chemical and of course PHY is physical. These are common types of foaming agents used industry. The final 2 numbers indicate the proportion of gelatinized starch based on weight percent.

Pre-polymer %	Gelatinized Starch %	Foaming Agent	Final Foam NCO/OH	Sample Name
90	10	none	1.0	ENDOPHY10
80	20	none	0.6	ENDOPHY20
70	30	none	0.4	ENDOPHY30
60	40	none	0.3	ENDOPHY40
50	50	none	0.2	ENDOPHY50
90	10	Sodium BiCarb., Citric acid, Stearic acid	0.9	ENDOCHEM10
80	20	Sodium BiCarb., Critic acid, Stearic acid	0.6	ENDOCHEM20
70	30	Sodium BiCarb., Citric acid, Stearic acid	0.4	ENDOCHEM30
60	40	Sodium BiCarb., Critic acid, Stearic acid	0.3	ENDOCHEM40
50	50	Sodium BiCarb., Citric acid, Stearic acid	0.2	ENDOCHEM50
90	10	Benzenesulfonly Hydrazide	1.0	EXOCHEM10
80	20	Benzenesulfonly Hydrazide	0.6	EXOCHEM20
70	30	Benzenesulfonly Hydrazide	0.4	EXOCHEM30
60	40	Benzenesulfonly Hydrazide	0.3	EXOCHEM40
50	50	Benzenesulfonly Hydrazide	0.2	EXOCHEM50

NOTE: Sodium BiCarb. is $NaHCO_3$

Table 2-Foam Nomenclature

IX. Characterization

12. Mechanical

Analysis of foam was simply achieved by addressing mechanical and physical properties of the foam. Mechanical properties include energy absorption, compressive stress, modulus and theoretical static shock cushioning. Physical properties include density, cell size and cell count. Data for mechanical analysis was collected on an Instron universal testing frame model 5567. The test frame was fitted with a 5kN load cell and # T489-74 compression platens rated for 100kN as seen below in figure-13

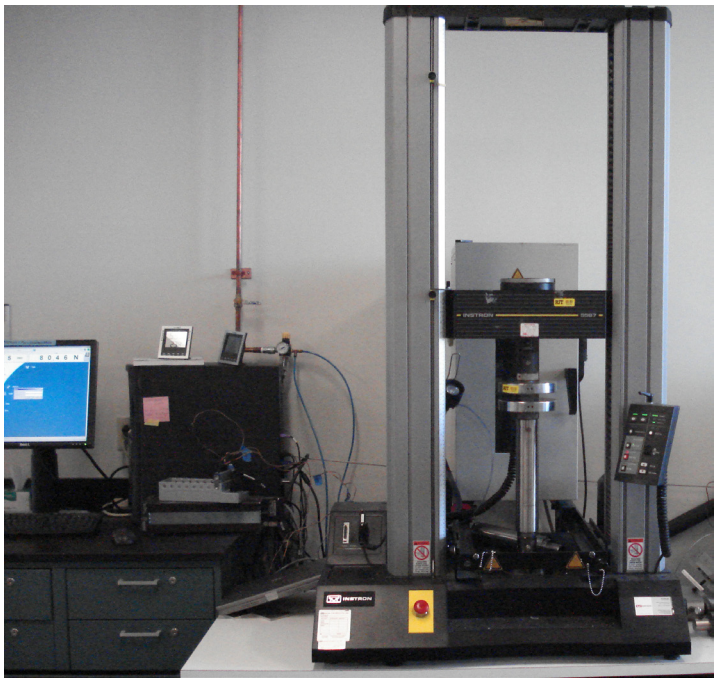

Figure 13-Compression test setup

The test frame is controlled with BlueHill™ 2 software. Compression data was collected in accordance to ASTM D3574. 13797 Standard test method for Flexi able Cellular Materials-Slab, Bonded Urethane Foams. Samples were compressed 16%, 32%, 48% and 68% of initial height at 100 mm/min. Samples were cut into cubes with dimensions 12.7 mm x 12.7 mm x 12.7mm ± 0.5 mm for all dimensions. For each type of foam 5 samples were tested. Data points collected include stress at each of the different strains loading and unloading energies, hysteresis, and compression modulus. Hysteresis was calculated by integrating top and bottom curves and taking the difference of the products. Samples were tested at ambient conditions in addition to 90% R.H. Samples

were conditioned in a Thermotron model SM-4-8200 environmental chamber at 23^{o}C and 90%R.H. for 24hrs. Compression in 2 different orientations perpendicular and parallel to the mold surface was completed for sample ENDOCHEM 40 to have an understanding on the effect of cell orientation and applied stress.

13. Physical

Density of foam was measured using on Ohaus Scout Pro SPE2001 analytical balance and Ohaus scale density determination kit and distilled water as the auxiliary

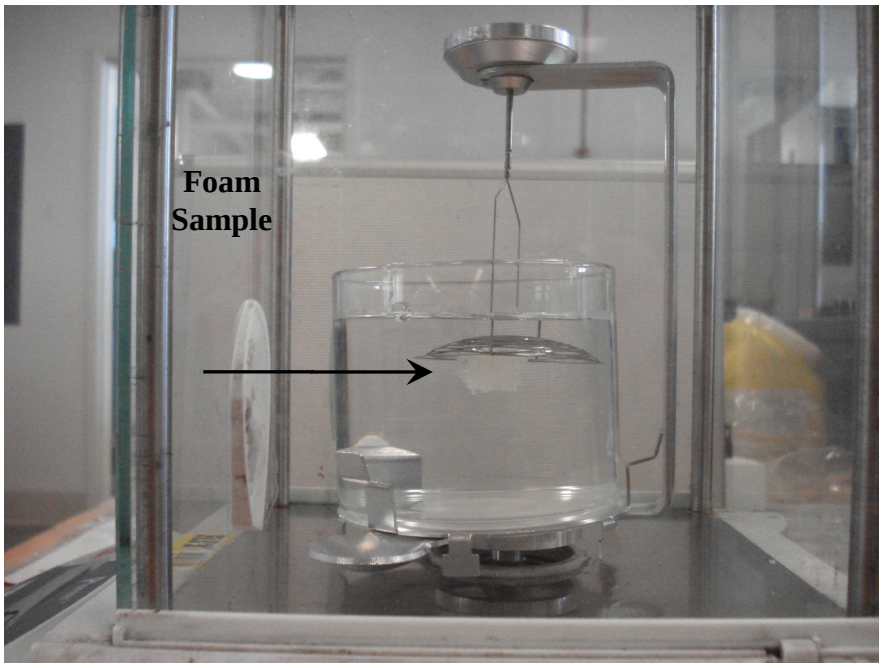

Figure 14-Density determination kit setup

liquid. The kit is designed around Archimedes principle of displacement seen in figure 14. A unique attribute of the apparatus is that it can measure the density of sample that typically floats in water or other liquid medium such as acetone. Archimedes principle states that the buoyant force of an object is equal to the weight of displaced fluid from the object Archimedes principle is found in equation 4. Here ρ is equal to sample density, A is equal to the sample weight in normal atmospheric conditions, b is equal to sample weight in liquid medium, distilled water in this case. ρ_o is equal to the density of water and ρ_L is the density of air.

Equation 4- Archimedes principle $$\rho = \frac{A}{A-b}(\rho_{0-}\rho_L) + \rho_L$$

Samples were cut into squares for each test and tested consisted of 10 samples for each different foam.

Cell size and cell count was measured using Metcal VPI-1000 Optical inspection system seen below in Figure-15. Pictures were taken at 35X magnification.

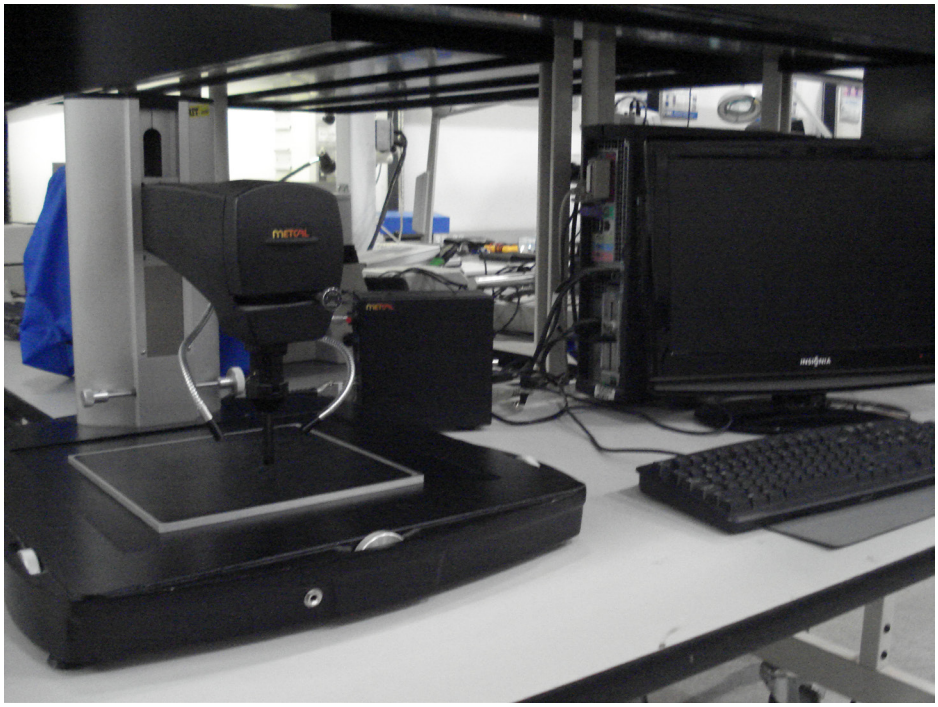

Figure 15-Optical measuring instrument

The software allows the user to trace the parameter edge of the cell, once tracing is complete cell area is automatically measured. Before testing a calibration of 1mm was made. Before placing samples under the microscope the surface of interest was colored black with a maker to make cells more apparent. 5 samples of each type of foam were measured. Data collection includes measurement of cell cross sectional area and number of cells in the overall cross section. A visual analysis of cell structure was performed as well. Samples view area was 11.2 mm x 8.4 mm.

14. Fourier Transform Infrared Spectroscopy (FTIR)

A spectrum of foam samples was collected to help understand discrepancies seen in mechanical properties or sample preparation. A PerkinElmer model Frontier FTIR spectrometer with the universal ATR accessory was used to collect sample spectra, seen figure 16. The instrument is equipped with Spectrum software. Each sample was scanned

5 times and peak detection was set to 0.30% transmission. Before sample testing samples were conditioned inside a convection oven at 70^{o}C for 24 hours to mitigate any effects of atmospheric moisture. Samples consisted of random section cuts from the overall foam.

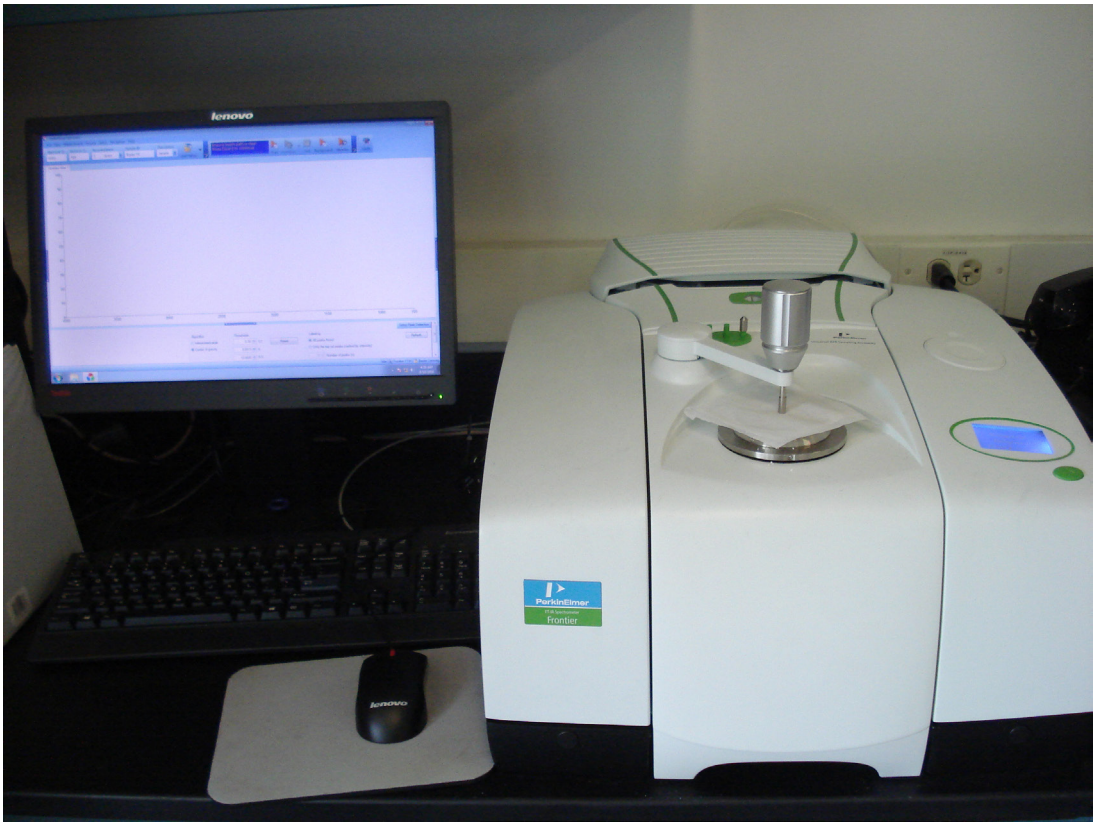

Figure 16-PerkinElmer Fourier transform Infrared Spectrometer with ATR accessory

X. Results and Discussion

15. Density

Foam density appears to be proportional with the amount of starch incorporated as seen in Figure 17 where the percentages indicate starch content. However there is non-consistent data for EXOCHEM samples at 20-30(%w/w) gelatinized corn starch. The densities seem to decrease from 20% to 30%. To try and understand any discrepancies another batch of samples were prepared and re-tested. The new EXOCHEM20 mean density decreased by 0.08 g/cm^3. However the standard deviation in density between new EXOCHEM20 samples is 0.06. Thus the difference between the old and new EXOCHEM20 samples is insignificant. And data most likely reflects an accurate trend in foam density. Furthermore, error bars indicate EXOCHEM20 samples can be created with a lower density than EXOCHEM30. Sodium bicarbonate, citric acid and stearic acid are the foaming agents used in EXOCHEM samples. Two plausible reasons for the discrepancy are: first, method of mixing the pre-polymer and gelatinized corn starch creates low dispersion and second, unknown chemical interaction occurs between the foaming agents and the blend constituents. Hence a cumulative effect may occur.

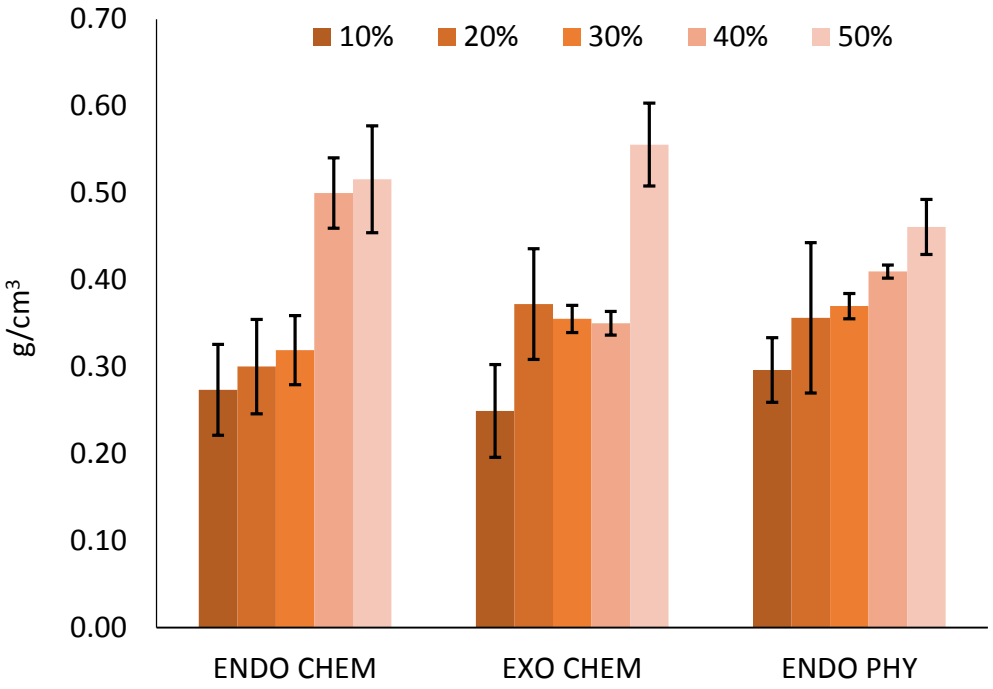

Figure 17-Foam Density

Plot #1 gives more insight into the relation of density and gelatinized corn starch content. It appears to be two different functions that govern the density of the foams. Each chemical foaming agent best follows a polynomial function. On the other hand the physical foaming agent closely resembles a linear relationship. Furthermore it is unclear which foaming agent may increase or decrease density of the final foam material in general.

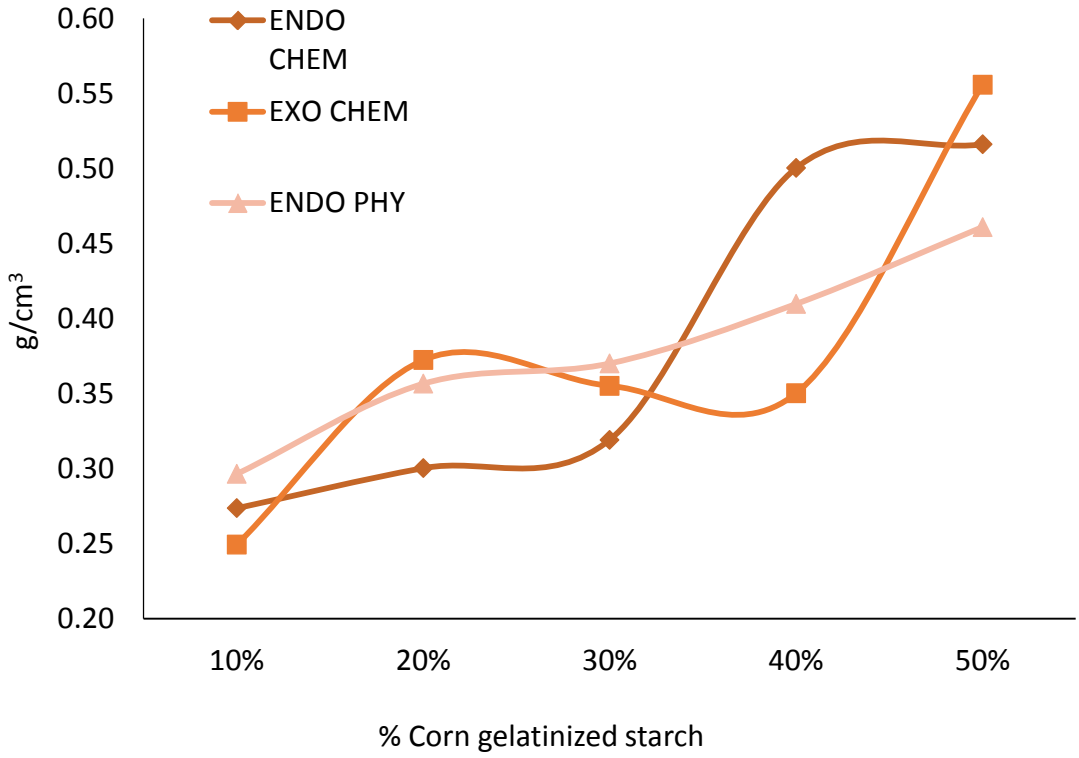

Plot 1-Density vs Gelatinized corn starch content

In Plot 2 both 20% and 40% gelatinized starch blends are removed. As seen below the effect of each foaming agent is evident. Since foaming agent concentration remained at 1(% w/w) for each blend, quantitative characterization is difficult and a qualitative approach is used. As mentioned earlier ENDOPHY samples follow a linear model and have a greater density than either chemical foaming agent. Once 30 (%w/w) gelatinized starch is exceeded EXOCHEM samples become denser and at 40(%w/w) both chemical samples show higher density than the physical foaming agents. After 20(%w/w) gelatinized starch content EXOCHEM samples appear to have a higher density than ENDOCHEM samples.

Over all removing 20 and 40 (%w/w) blends from the plot yielded a coefficient of determination of 1 for both chemical foaming agents and 0.99 for the physical foaming agent increasing model accuracy. Due to the difference in plots 1 and 2 an initial assumption is that the blending process appears to have a low shear rate and thus poor dispersion between the pre-polymer and gelatinized starch. Differentiating between blends with 10% change in gelatinized corn starch as seen in plot 1 can be misleading.

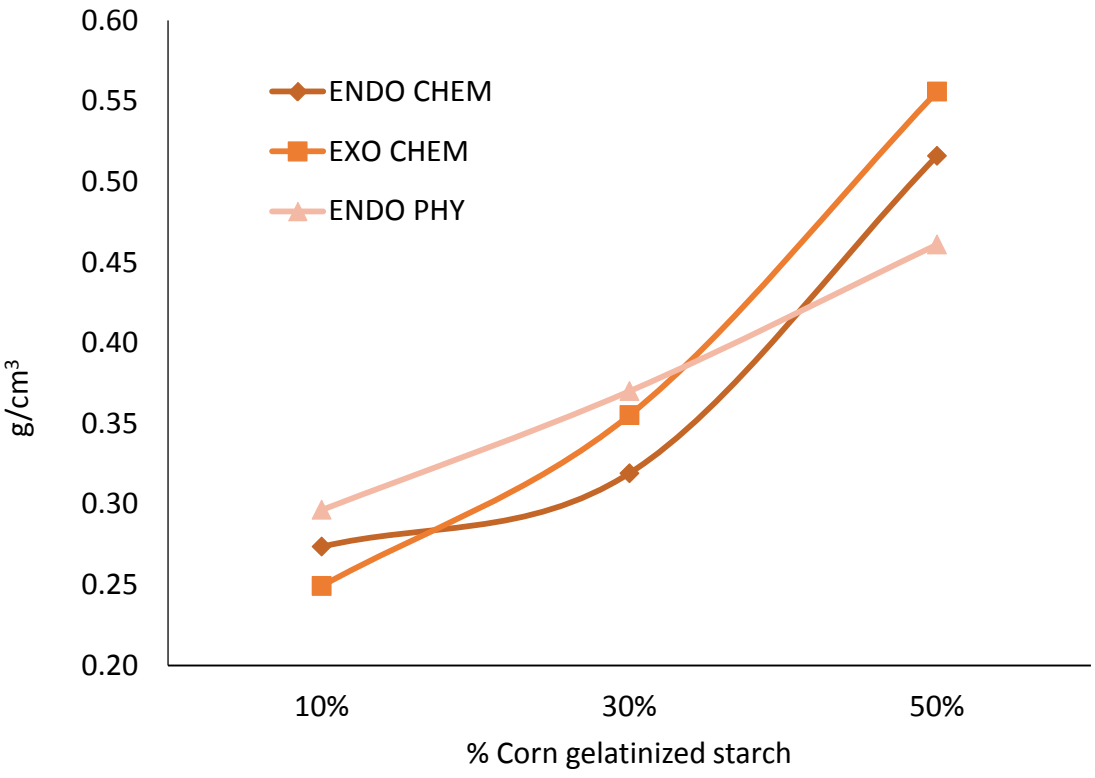

Plot 2 - Density vs. Gelatinized corn starch content with samples 30% and 40% removed

In published literature other researchers have measured similar densities. As seen in Table 3 examples 2-4 coincide with the above results. The densities within this research range from 0.25 to 0.55 g/cm^3.

	Author	Density (g/cm^3)	Material
1	by Mosiewicki, A. M., et. al. (2009)	0.037-0.038	Foam
2	Wang, J, H., Rong, Z, M., Zhang, Q, M., Hu, J., Chen, W, H., and Czigany, T. (2007).	0.12-0.35	Foam
3	Wang, C., Zheng, Y., Xie, Y., Qiao, K., Sun, Y. and Yue, L. (2015).	.102-.219	Foam
4	C. and Skala, M. D.(1997).	0.1-0.4	Foam

Table 3-literature review density

16. Cell Count

When examining the effect that gelatinized starch content has on foaming agent performance, cell count and cell cross sectional area are able to provide insight. Immediate differences in cell count and mean size are noticed between both chemical and physical foaming agents. For ENDOPHY foam samples a polynomial function is able to be found describing the relationship between cell count and gelatinized starch content as seen in plot 3. As gelatinized starch content increases the number of cells also increases. Seen below in Figure 18 are ENDOPHY10 on the left and ENDOPHY50 on the right, each surface was colored with black ink to help differentiate between the surface and cell. Mean cell counts are 25 and 37 respectively. Mean cross sectional cell areas are 1.8 and 0.9 mm^2 respectively.

Cell geometry indicates coalescence and open cell structure. Where the larger cells are circular in shape and the smaller cells appear to be elongated voids. On the other hand ENDOCHEM and EXOCHEM foams show a slight relationship between cell count and content of gelatinzed starch. As gelatinized starch content increases the cell count decreases for both EXOCHEM and ENDOCHEM samples. For ENDOPHY samples cell content increases, presumably because there is more gelatinized starch content and thus water content to create a increased foaming affect.

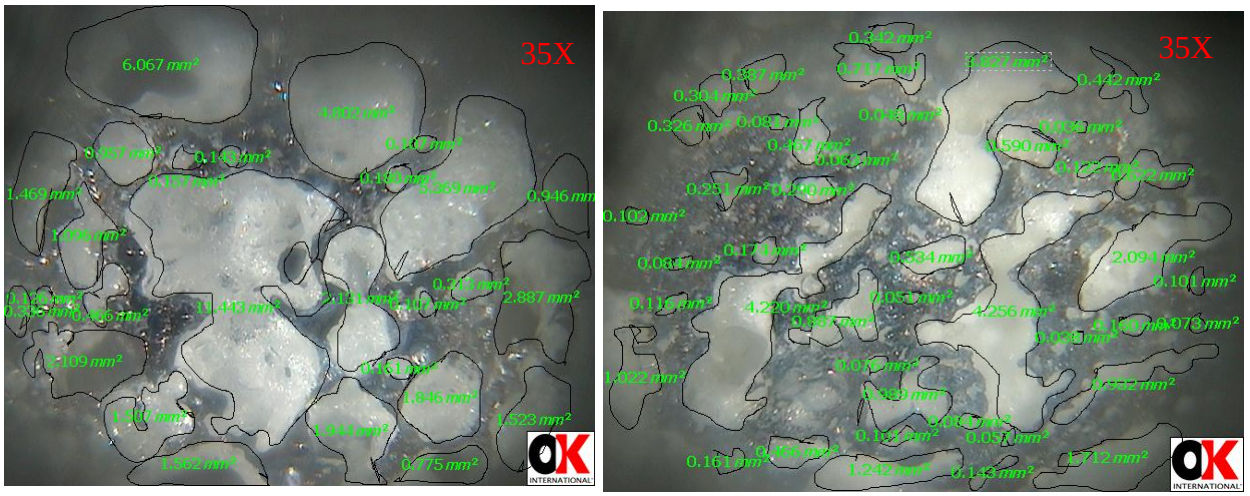

Figure 18- ENDOPHY10 AND ENDOPHY 50

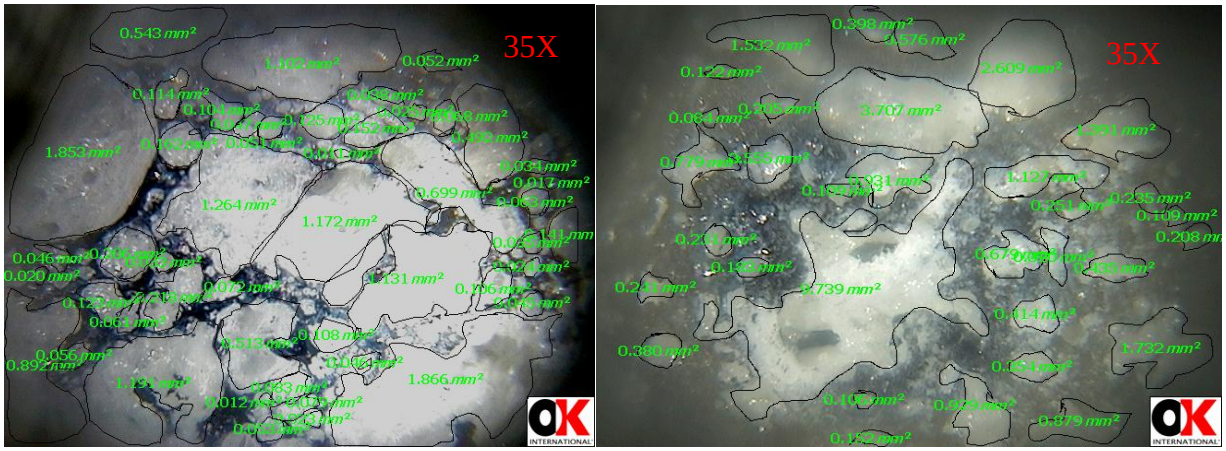

Figure 19-ENDOCHEM10 AND ENDOCHEM50

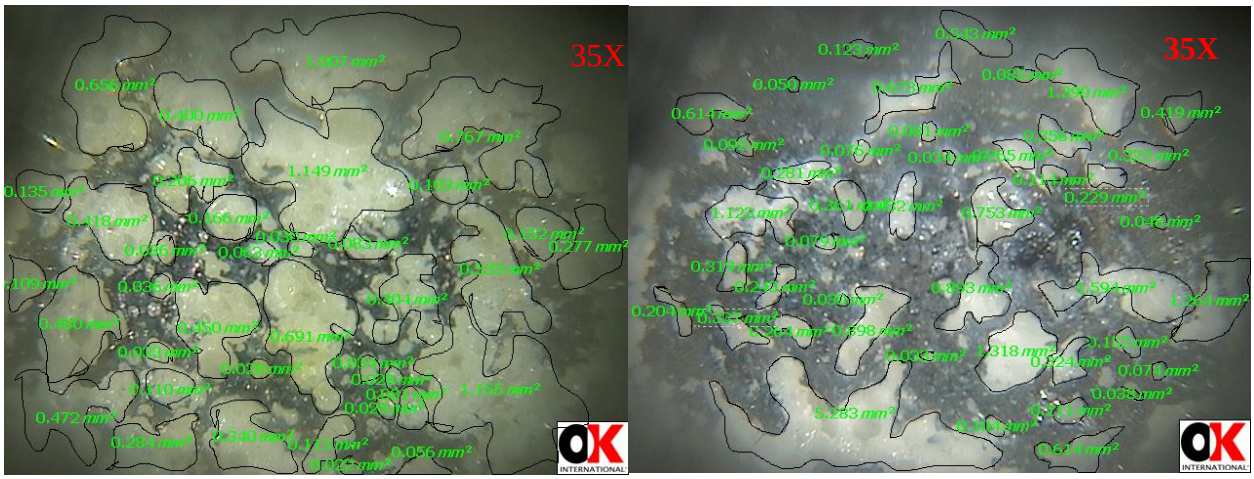

Figure20-EXOCHEM10 AND EXOCHEM50

Cell count and gelatinized starch content appear to be associated as seen in plot 3 below. Both chemical foaming agents show a peak cell count of 50 cells at around 20 (%w/w) gelatinized corn starch whereas a physical foaming agent yields a high cell count of 35 cells at 50 (%w/w) gelatinized cornstarch. Least cell counts for each chemical foaming agent differ. EXOCHEM30 samples have the least count of cells at 19 cells and ENDOCHEM40 samples had the least number of cells at 24.

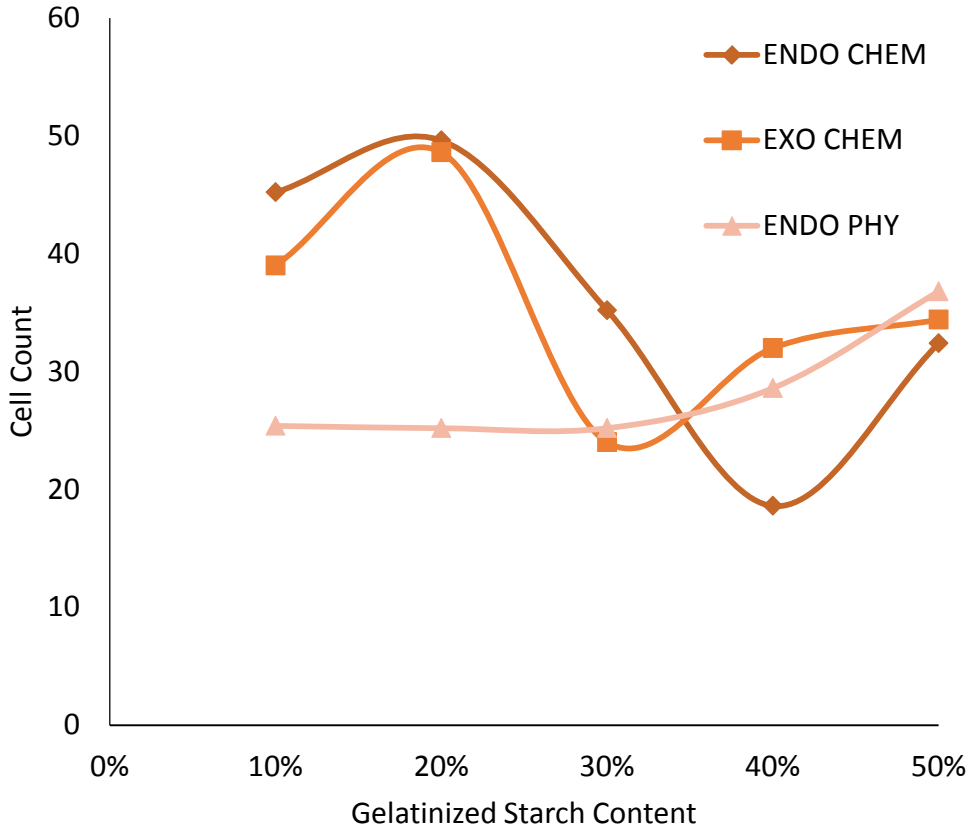

Plot 3 - Cell count vs. Gelatinized starch content

A neat pattern is observed with mean cross-sectional area in plot 4. Each foam sample has a peak mean cell size of $> 2.0\ mm^2$ but at different gelatinized starch concentrations; ENDOCHEM cell cross sectional area peaks at close to 40(%w/w), EXOCHEM at 30(%w/w) and ENDOPHY at 20(%w/w) gelatinized starch. After each of the different foams reach the peak a continous drop in cell-cross sectional area occurs, most notably with the ENDOPHY samples. Furthermore a comparison of plots 4 and 5 indicates that as cell size increases, the number of cells decreases, in other words reciprocal relationship typically noticed in foamed materials. In comparison to figure 16 as gelatinized starch content increases density simultaneously increases regardless of the foaming agents used.

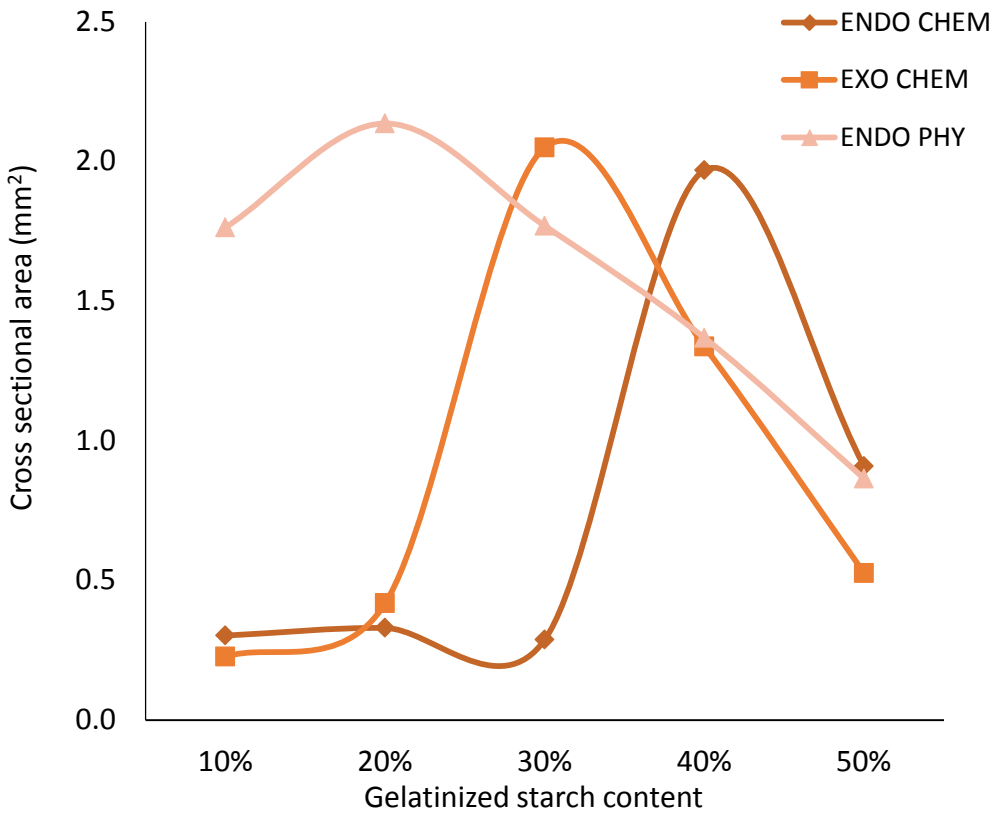

Plot 4-Cell cross sectional area versus Starch content

Plot 5 below shows the relationship between cross sectional cell area and number of cells. For each foam the cell count ranges from 19 to 50 cells. The cross sectional area ranges from 0.2 mm^2 to 2.0 mm^2. Cell coalescence is more likely to appear at lower starch concentations than at high concentrations. This is evident by changes in viscosity when mixing gelatinized starch and prepolymer. At low concentrations of gelatinized starch viscosity is low and coalescence more likely to occur. Whereas when viscosity increases cell shape is retained but also more likley to collapse. The assumpation also follows along with why samples with higher gelatinized starch content have lower cell cross sectional area because the pressure exerted from the foaming agent on the blended materials is constricted by blend viscosity.

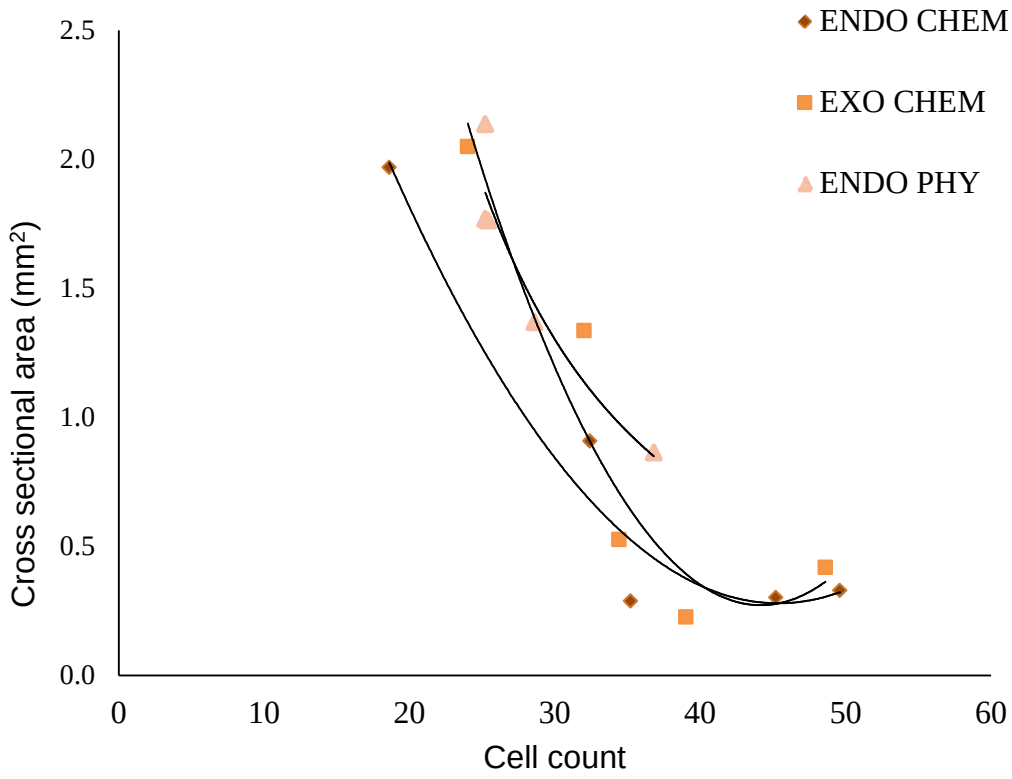

Plot 5-Mean cell x-section vs starch content

17. Compression and Energy Absorption

Compression results are interesting and do not show a clear trend in regards to gelatinized starch content. Mechanical properties measured: stress at maximum strain, hysteresis, modulus and theoretical static cushion curves were derived. Samples were tested at 4 different strains, high humidity and ambient atmospheric conditions. After testing the samples were observed to make nearly a full recovery to initial dimensions, but as strain increased time to recovery greatly increased. Furthermore the maximum strain of 68% is approaching threshold for permanent deformation.

Per figure 20 perpendicular refers to foam being compressed perpendicular to direction of rise and parallel refers to the compression force being uniaxial with direction of rise. In other words compression platens are parallel with the natural surface of the foam. It appears that foams show isotropic behavior at 50% strain. It should be noted that the variation in compression properties due to direction of the foam is not taken into consideration in proceeding tests. The reason being that the method used for mixing gelatinized starch and pre-polymer creates poor dispersion or unknown interactions of materials and is thought to be the main cause for variation in results. As seen below the standard deviation for each sample overlaps one another. During compression tests similar behavior was observed with all samples; with respect to either perpendicular or parallel direction stress measured can be randomly high or low within that given range.

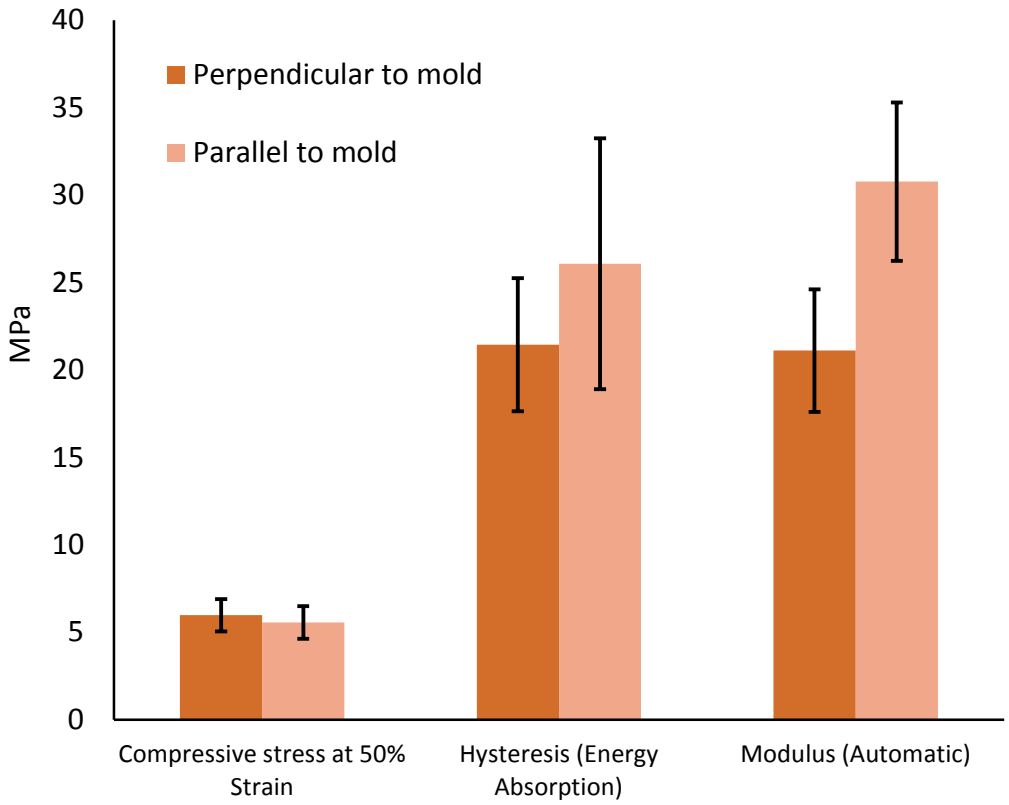

Figure 21-ENDOCHEM40 direction dependent properties at 50% strain

Figure 21 shows the compression modulus at 16% strain for all samples. At first look results appear to have an erratic trend, but both ENDOCHEM and ENDOPHY have a peak stress of 22 and 24 MPa respectively at 40(%w/w) gelatinized starch. At 40(%w/w) gelatinized starch there could be a critical point for the interactions between gelatinized starch and pre polymer. Densities measured would suggest the densest samples would yield the highest modulus, however weak interactions within the macromolecule structure could cause sample failure before the full strain is reached. It should also be noted that samples did not become fragmented after compression. Overall the moduli can vary by a factor of 10, dependent on gelatinized starch content or foaming agent.

In comparison to figure 22 the moduli increase substantially due to higher strains but overall the trend is similar. The error bars represent the standard deviation between samples that were prepared completely at random orientation with regards to figure20. It may indicate poor dispersion as noted earlier.

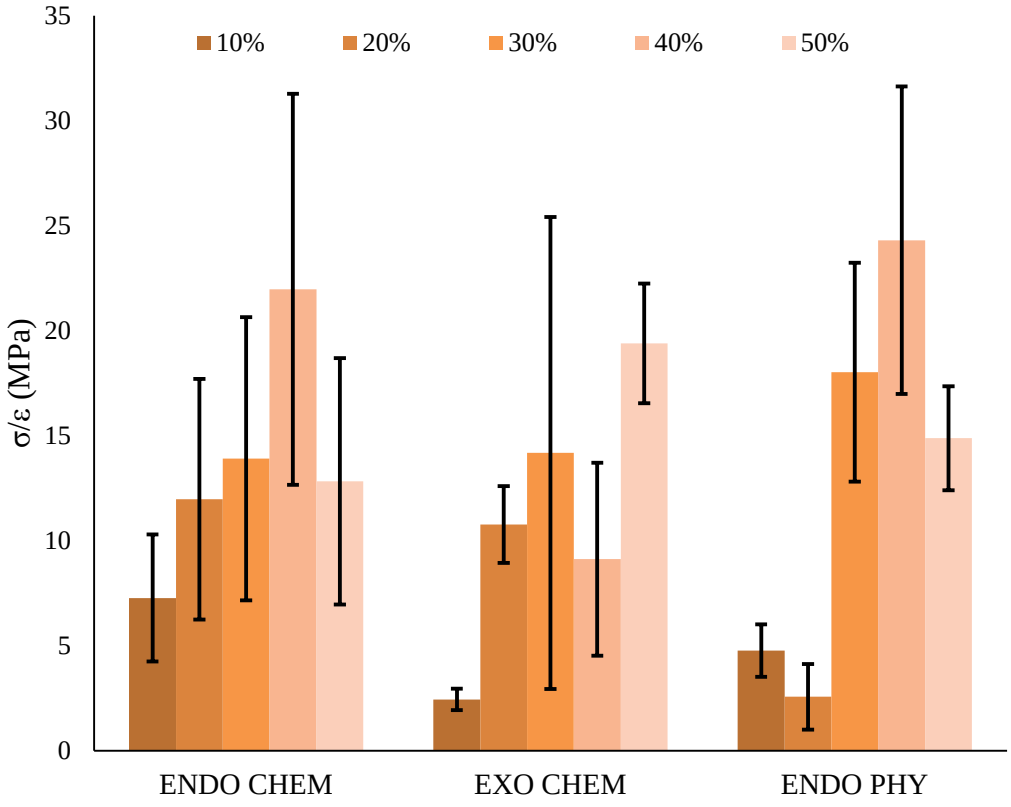

Figure 22-Compression modulus results at 16% strain

The compression modulus of each material at 68% strain is found in Figure 22. Set of samples for each different type of foaming agent show different trends. In general however increase in gelatinized starch content causes modulus to increase.

For ENDOCHEM samples 10-30 (%w/w) show little change in modulus even with changes noted above in cell structure. The change from 30(%w/w) to 40(%w/w) appears to increase by a factor of 2 or more. For EXOCHEM samples the moduli change by a factor of 7. EXOCHEM20-40 have similar moduli ranging from 34 to 38 MPa. And EXOCHEM50 has a maximum modulus of 75 MPa. Finally ENDOPHY samples have the most discernable trend; as gelatinized corn starch content increases modulus proportionally. Contrasting ENDOCHEM and EXOCHEM with ENDOPHY samples suggest that foaming agents affect foams modulus but in contrast to 16% strain it is believed that gelatinized starch is a major factor for 50% samples below in Figure 22.

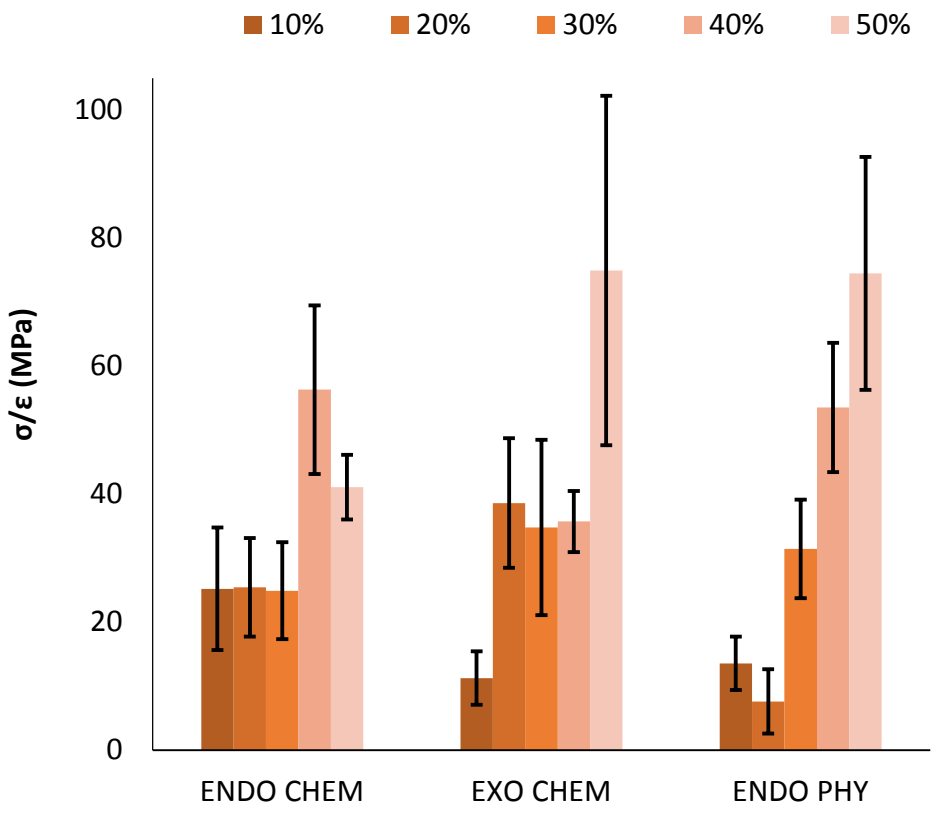

Figure 22-compression modulus at 68% Strain

To help determine how foaming agents may affect modulus plot 6 below shows the relationship between cell size vs compression modulus. These findings agree in 2 ways with plot 4; cross-sectional area vs gelatinized starch content. First, cross sectional area decreases when both gelatinized starch content and modulus increase for ENDOPHY samples. Second, both foam samples made with chemical agents show opposite trends than the single physical foaming agent.

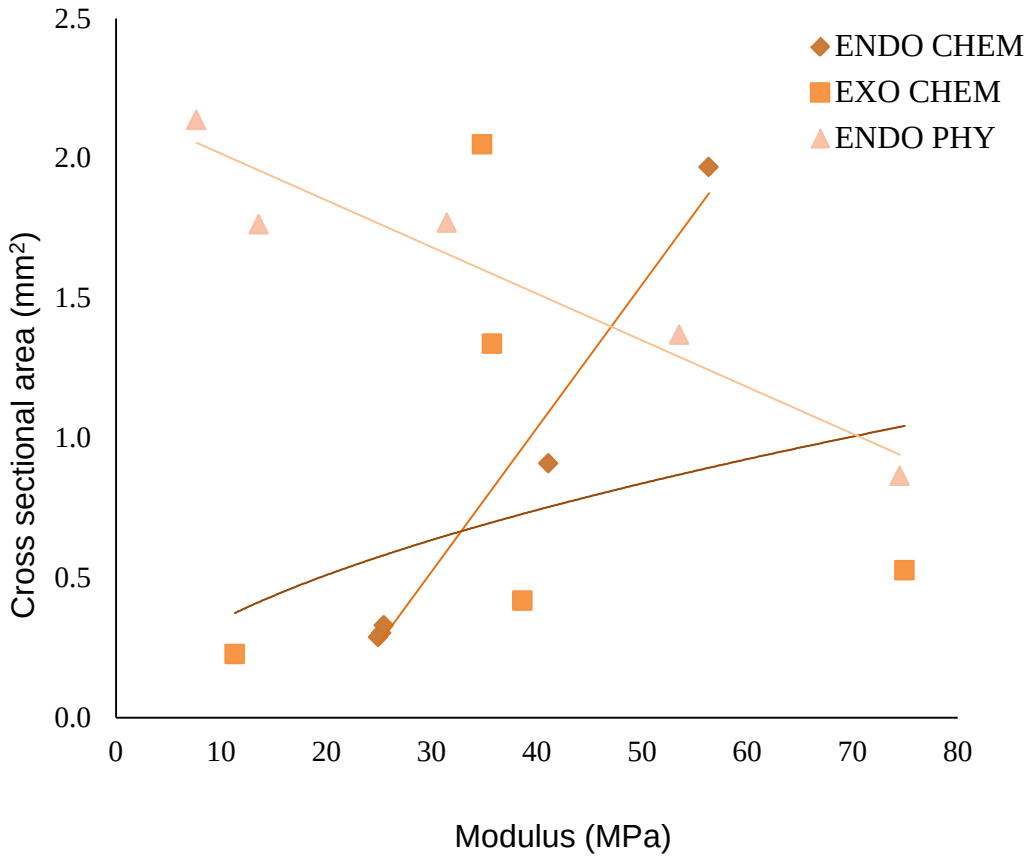

Plot 6- Cell Size vs. Modulus at 68% strain

In literature review starch based materials are noted extensively for their hydrophilic behavior. Samples were conditioned in both ambient conditions and at 90% R.H. and 23^{o}C and then compression tested. Results in plot 7 show 3 logical trends. First; each set of samples ranging from 10-20(%w/w) appear to measure the same stress at 50% strain regardless of previous conditioning. Second, from 20-40 (%w/w) ambient conditioned samples measured higher static stress and third samples with 40 to 50 (% w/w) gelatinized starch conditioned at 90% R.H see a greater increase is stress. This switch in behavior indicates that not only does the foam become stronger but there are interactions between the foamed materials and a humid environment.

Furthermore significant changes in compression stress are observed at 50 (% w/w) gelatinized starch for all samples. EXOCHEM50 samples show the greatest increase in compression stress; from 6 MPa for ambient conditioned samples to 12 MPa for 90% R.H. conditioning, increasing by a factor of 2 may indicate changes in the chemical structure or secondary interactions with the environment. ENDOCHEM50 samples show a 60% compression stress increase and ENDOPHY50 sample have 50% compression stress increase. According to Table 4 -OH- molarities are 0.51 for EXOCHEM10 and EHNDOPHY10 samples and 0.54 ENDOCHEM10 samples. The molarity for NCO used to prepare samples is 0.52. Thus samples with approxiamately10 (%w/w) gelatinized corn starch have the highest probability of optimal interactions within the blend itself and outside factors such as high humidity should have little to no effect on blends. Once the moles -OH-surpass 0.52 interactions with a humid environmental evident by changes in plot 7.

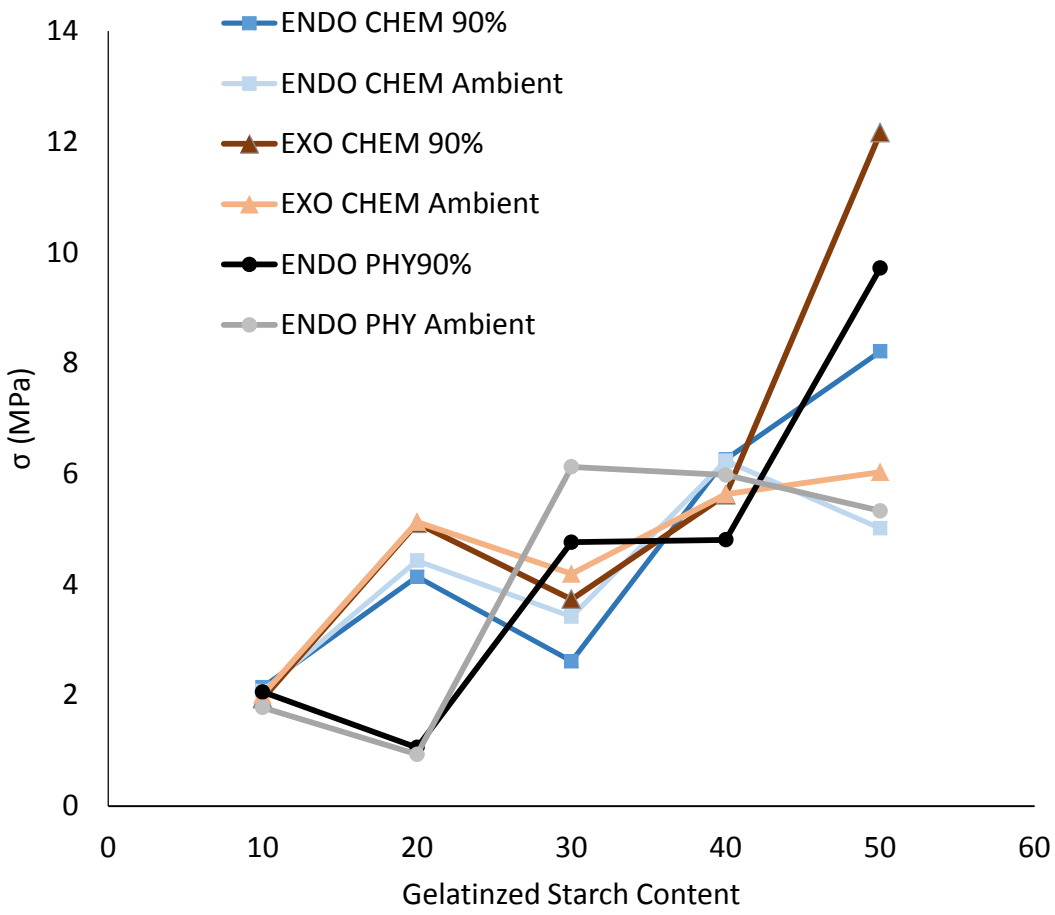

Plot 7- Effect of humidity on compression stress at 50% strain

18. Cushion curves

Developing cushion curves for foam is a preliminary task to developing through-mail packages or for a dynamic environment. Creating cushions curves for these foams can help differentiate between which foams can be useful or further optimized via equation 3. Actual testing requires large square samples of roughly 200 mm^2 and thus requires different sample preparation equipment which is unavailable. Calculated static cushion curves cover a wide range of product frigidly numbers at only 12 in drop height and appears to have no consistent trend between each different foaming agent. Validation of these cushions curves may result in a static cushion curve factor so that predicted values better match actual results (50). Gelatinized corn starch content on the other hand appears to cause a shift for each different foaming agent. To present a clear interpretation 20 and 40 (%w/w) gelatinized starch samples are removed from the plots below. Plots with all samples are in the appendix.

For all samples containing 10 (% w/w) gelatinized starch plot 8 shows predicted cushion curves. Both ENDOPHY and EXOCHEM have limiting G-values at 50% strain around 2 MPa. ENDOCHEM samples in comparison are limited at 50% strain but at a lower G-value. Overall the different foams can be utilized from 10 to 65 G-force and 0 to 2 MPa of stress.

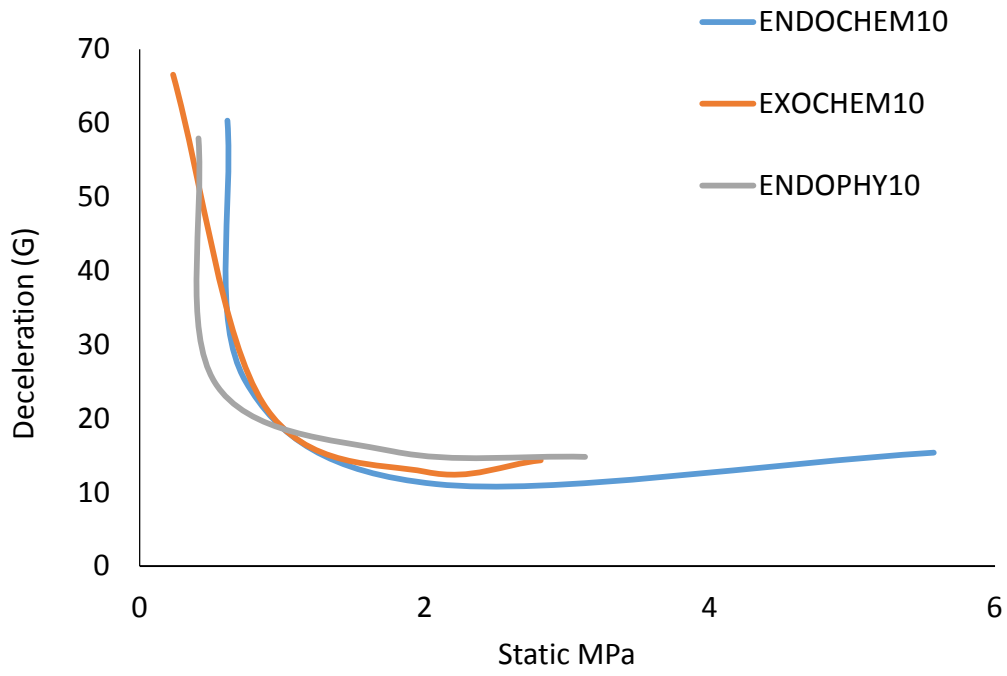

Plot 8-12inch static cushion curves for 10% gelatinized starch samples

As seen in plot 9 30 (%w/w) gelatinized corn starch product fragility increases to a range of 14 to 75 G's and a static stress range of 1.3 to 5 MPa. The increase over 10 (%w/w) gelatinized corn starch samples is most likely in agreement with preceding results. Gelatinized starch content increases foam modulus and thus energy density for shock absorption behavior. However shape or shift in curves between 10 and 30 (%w/w) gelatinized starch foams is peculiar. ENDOCHEM curves for both 10% and 30% are very similar in shape and coordinates. EXOCHEM and ENDOPHY samples at 10% actually behave better in terms of deceleration below 10 G's and sustain higher static stress than samples at 30%.

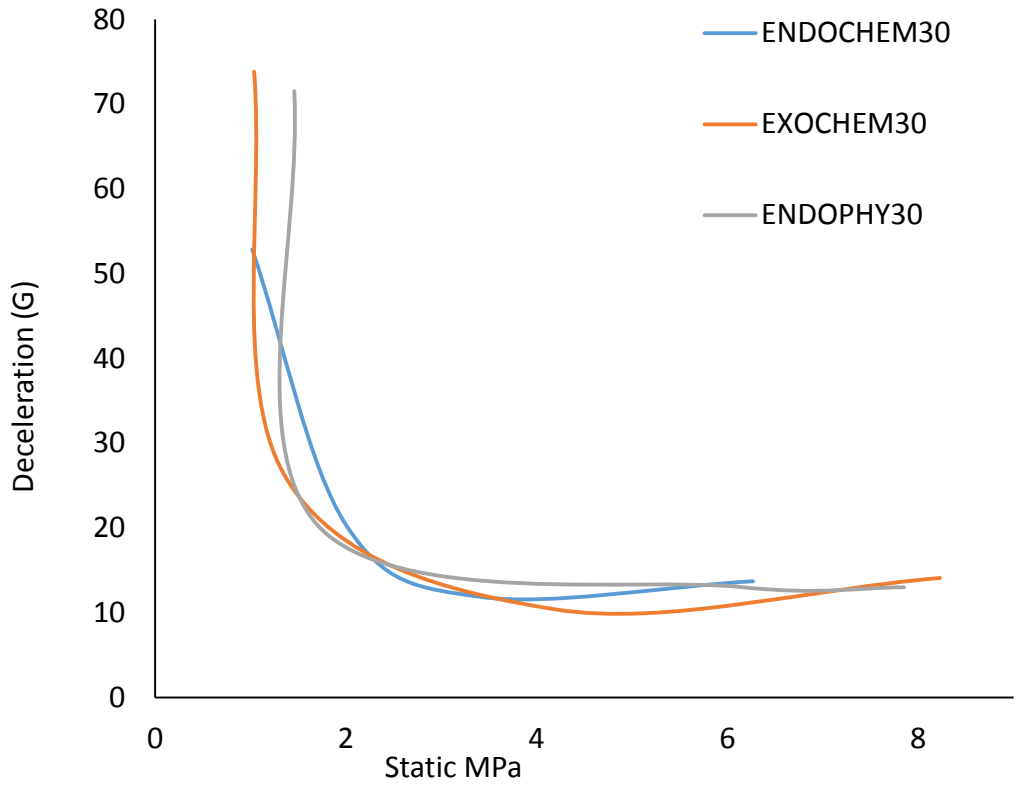

Plot 9-12inch static cushion curves for 30% gelatinized starch samples

For 50 (%w/w) gelatinized starch samples seen in plot 10 the limiting fragility values range from 14 to 75 G's. In contrast to the 30 (%w/w) samples there is little variance in deceleration. However the static stress values have an increase in range from around 2 to 18 MPa.

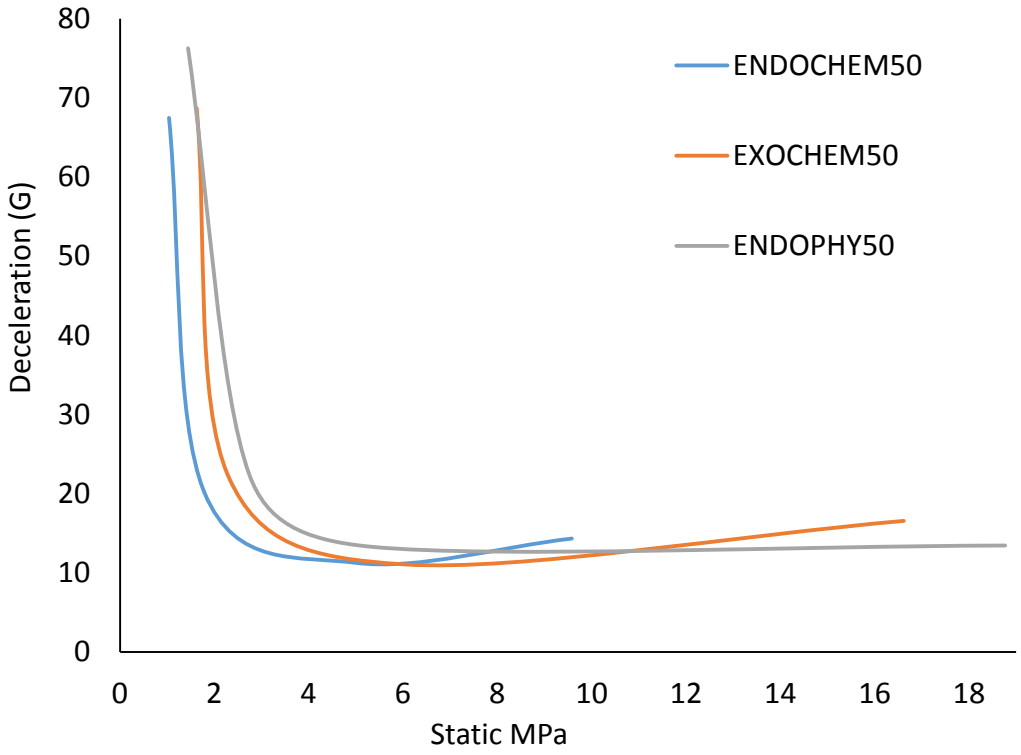

Plot 10-12inch static cushion curves for 50% gelatinized starch samples

Plot 11 plots the same foaming agent with different amounts of gelatinized starch. Shifts in the cushion curves are observed in contrast to previous plots that were based on different foaming agents. These plots clearly show the effect of gelatinized starch content on cushion performance. Each plot below excludes 30 and 40 (%w/w) gelatinized starch foams in an effort to more clearly understand results. The appendix has plots with cushion curves with all foam samples made.

EXOCHEM samples below in plot 11show a shift in static stress of about 1 MPa as the gelatinized starch content increases from 10 to 30 (%w/w) and finally 50(%w/w). Deceleration remains constant between samples with a threshold just above 10 G's at minimum.

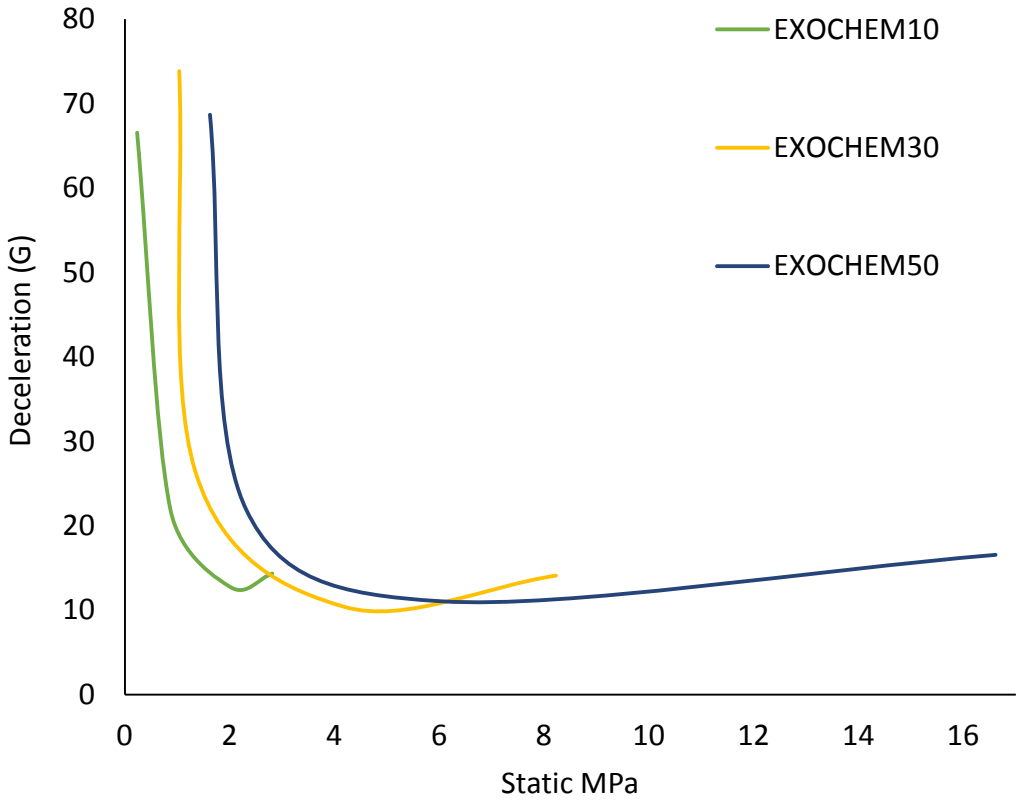

Plot 11-12inch static cushion curve for EXOCHEM foam samples

ENDOCHEM samples in plot 12 show a slight shift of 1 MPa in static stress after 10 (% w/w) gelatinized starches. However ENDOCHEM30 and ENDOCHEM 50 are fairly similar in behavior. Only differing by gelatinized starch content and ENDOPHY samples exhibit 20 G's deceleration at the same stress. ENDOCHEM 50 also has 54% more energy absorption at lower the deceleration threshold. The similarity between 30 and 50% gelatinized starch suggest that the materials dispersion may be interfering with material performance and in this case hindering them. With respect to plot 11 and 13, EXOCHEM and ENDOPHY samples show a clear shift with increased gelatinized starch content. For plot 12 the only difference would be the type of foaming agent incorporated. In addition to previous characterization methods plot 12 also suggest dispersion between materials in reference to samples ENDOCHEM30 and ENDOCHEM50.

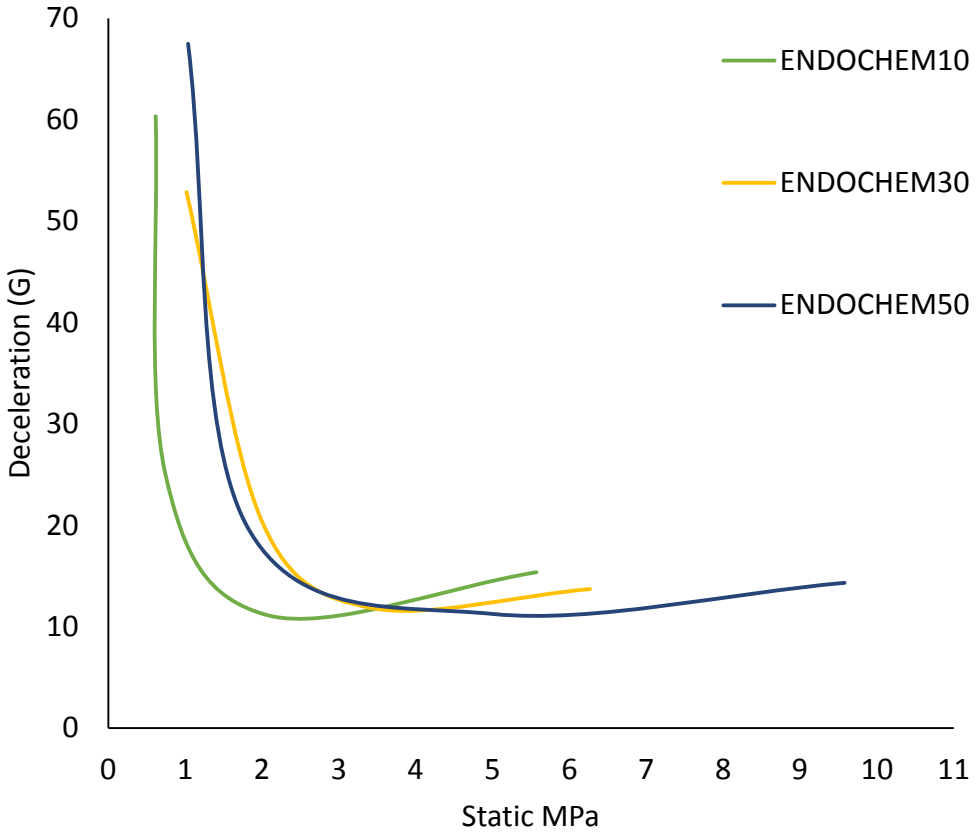

Plot 12-12 inch static cushion curve for ENDOCHEM foam samples.

For ENDOPHY samples in plot 13 much like EXOCHEM samples a shift is noticed. As gelatinized starch content increases a higher stress at nearly the same deceleration is found. And overall having a greater stress range than the 2 previous samples at 50 (%w/w) gelatinized starch. Each of the ENDOPHY samples reaches minimum deceleration of 13-14 G'. In contrast to ENDOCHEM there appears to be a strong influence of gelatinized starch content which also brings to light possible interactions between chemical foaming agents and the material blend.

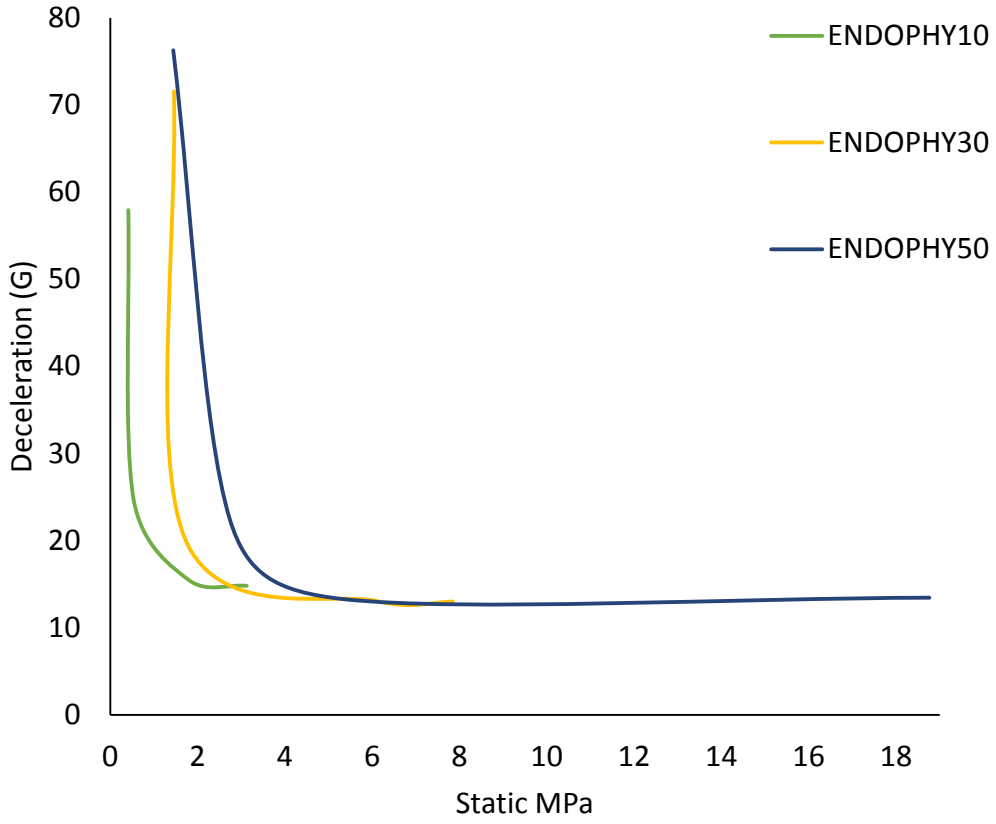

Plot 13-12 inch static cushion curve for ENDOPHY foam samples

19. Fourier Transform Infrared Spectroscopy (FTIR)

ENDOPHY samples seen in figure 23 appear to have immediate change in spectrum intensity from ENDOPHY10 to all foam samples with higher percent gelatinized corn starch. The ENDOPHY10 spectrum wave number 1715-1717 cm^{-1} and 1509 to 1519 cm^{-1} is suspected to be a -N-H- that has hydrogen bonded with -OH- groups of both castor oil and gelatinized starch. With the incorporation of additional isocyanate segments potential interactions between the prepolymer and gelatinized corn starch is anticipated. Furthermore evidence of free or non-reacted isocyanate segments would show a peak in the range of 2200-2400 cm^{-1}. The decrease in intensity in the remaining four samples is most likely caused by the increase in gelatinized starch content. Castor oil is identified at 2925-2854 cm^{-1} where -C-H- segments are stretch and bending. Furthermore the cis isomer in castor oil is identified at 722 cm^{-1}.

From an overall perspective there is no indication of starch in native form as would be indicated by a peak in the range of 3000-3500 cm^{-1}, where CH_2 shows bending absorption. ENDOPHY10 spectrum has peak at 3337 cm^{-1} with low intensity which suggests inconsistency in the gelatinization process. Furthermore a characteristic peak is missing in samples ENDOPHY20 and ENDOPHY50; 1045 and 1017 cm^{-1}. These peaks are in the fingerprint region and perhaps explain why mechanical properties have an erratic trend.

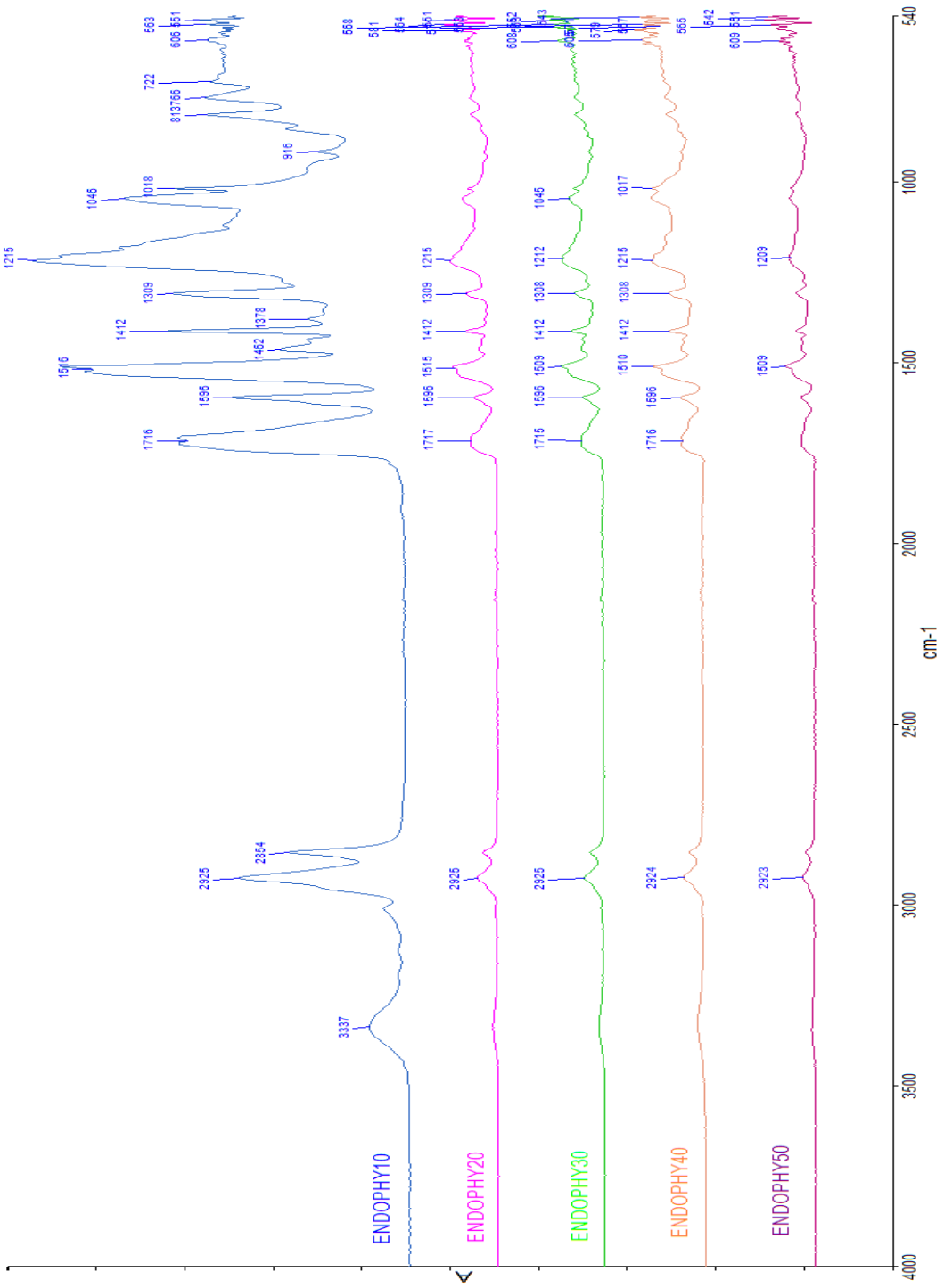

Figure 23-ENDOPHY FTIR-ATR Spectra

ENDOCHEM samples in figure 24 below have no immediate shifts in spectra, but subtle shifts are noticed in the range of 2922 to 2924 cm^{-1}. As mentioned previously these shifts can be associated with C-H in castor oil and CH_2 in corn starch. Evidence of native starch is indicated roughly in the range of 3000-3500 cm^{-1}, the stretching of hydroxyl groups. Broad peaks are noticed roughly at 3300 cm^{-1} with minimum intensity. Thus the wave numbers 2922-2924 cm^{-1} are designated as castor oil. As seen with ENDOPHY samples 2 peaks; 1715- 1717 cm^{-1} and 1509-1515 cm^{-1} show isocyanate interactions with both castor oil and starch respectively. Residual sodium bicarbonate is observed at roughly 1307-1308 cm^{-1} and from 1211-1213 cm^{-1} is residual citric acid (53).

To help describe the erratic trend in figures 21 and 22 peaks found in the range of 1713 to 1715 cm^{-1} could be the result of free and bonded urethane groups. From literature review a decrease in wave number correlates to hydrogen bonded urethane groups whereas a higher number is the result of free urethane groups. Thus in figure 22 ENDOCHEM 40 exhibits a maximum modulus due to increased intermolecular interactions.

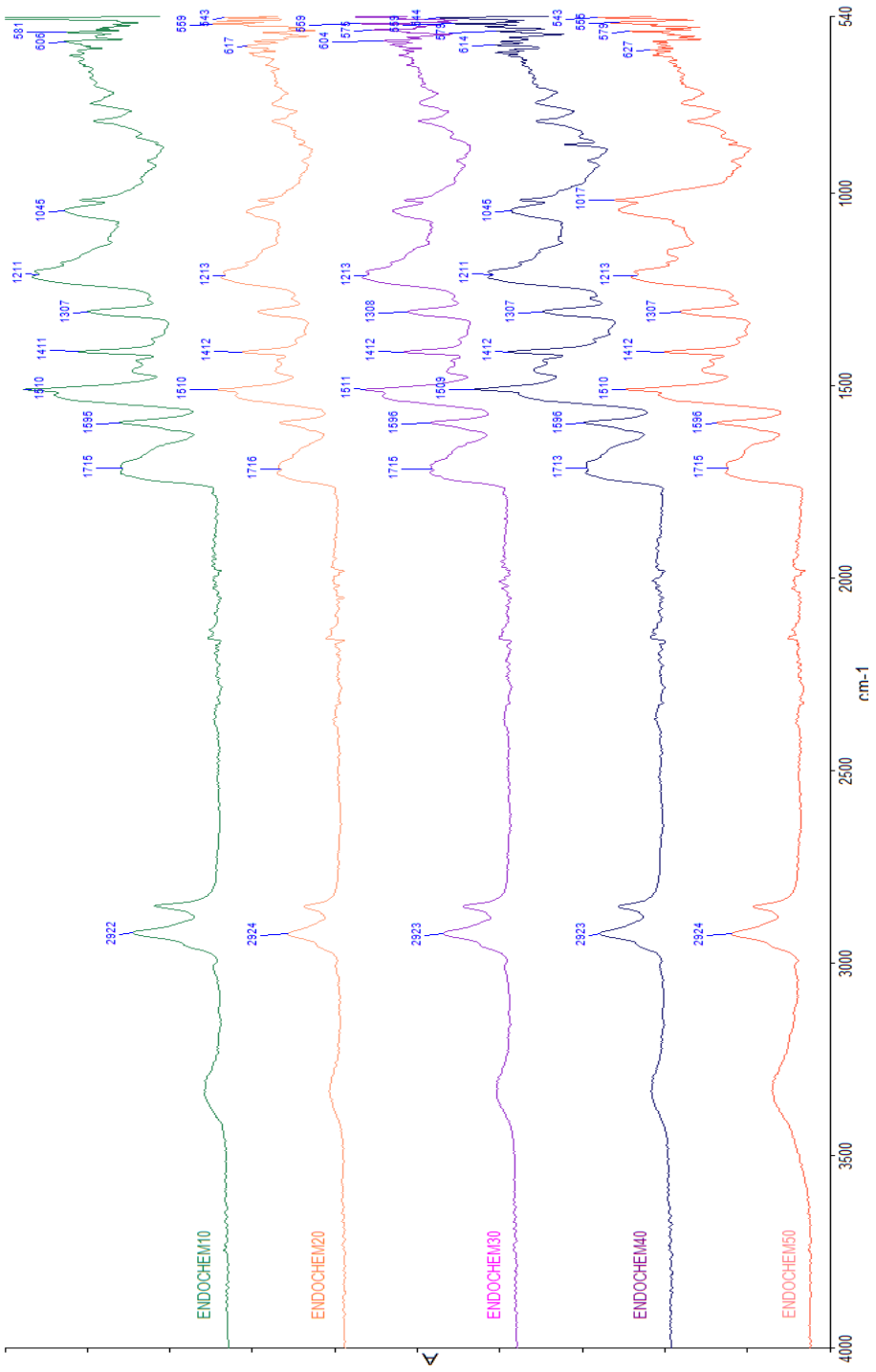

Figure 24-FTIR-ATR ENDOCHEM samples

The low intensity humps found in figure 26 between 3500-3000 cm^{-1} are evidence of native starch but not in its native form All EXOCHEM samples have the designated castor oil peaks at 2924-2925 cm^{-1} and 2854 cm^{-1}. Evidence of interactions between gelatinized corn starch, castor oil and urethane linkages is found at 1709 -1730 cm^{-1} and 1510-1511 cm^{-1} which is the formation of a saturated carbon atom a when a urethane linkage is created.

In regards to figure 22 (68% strain modulus bar graph) EXOCHEM20 has the highest modulus (40MPa) among samples EXOCHEM30 and EXOCHEM40. The spectra from EXOCHEM20 indicate poor blending/dispersion with a broad hump at 3333 cm^{-1} and free isocyanate segments at 2295 cm^{-1}. Furthermore the peak at 1720 cm^{-1} is the least intense among all 3 samples suggesting that the reaction preference was for castor oil over gelatinized corn starch. It is suspected that mixing of gelatinized corn starch and prepolymer was more thorough for EXOCHEM30 and EXOCHEM40 based on peak intensity at 1730 and 1718 cm^{-1} respectivly (increase in viscosity was observed). The intermittent double peak at 1017cm^{-1} and 1045 cm^{-1} are evidence of an aromatic ring and C-O-C segment respectively.

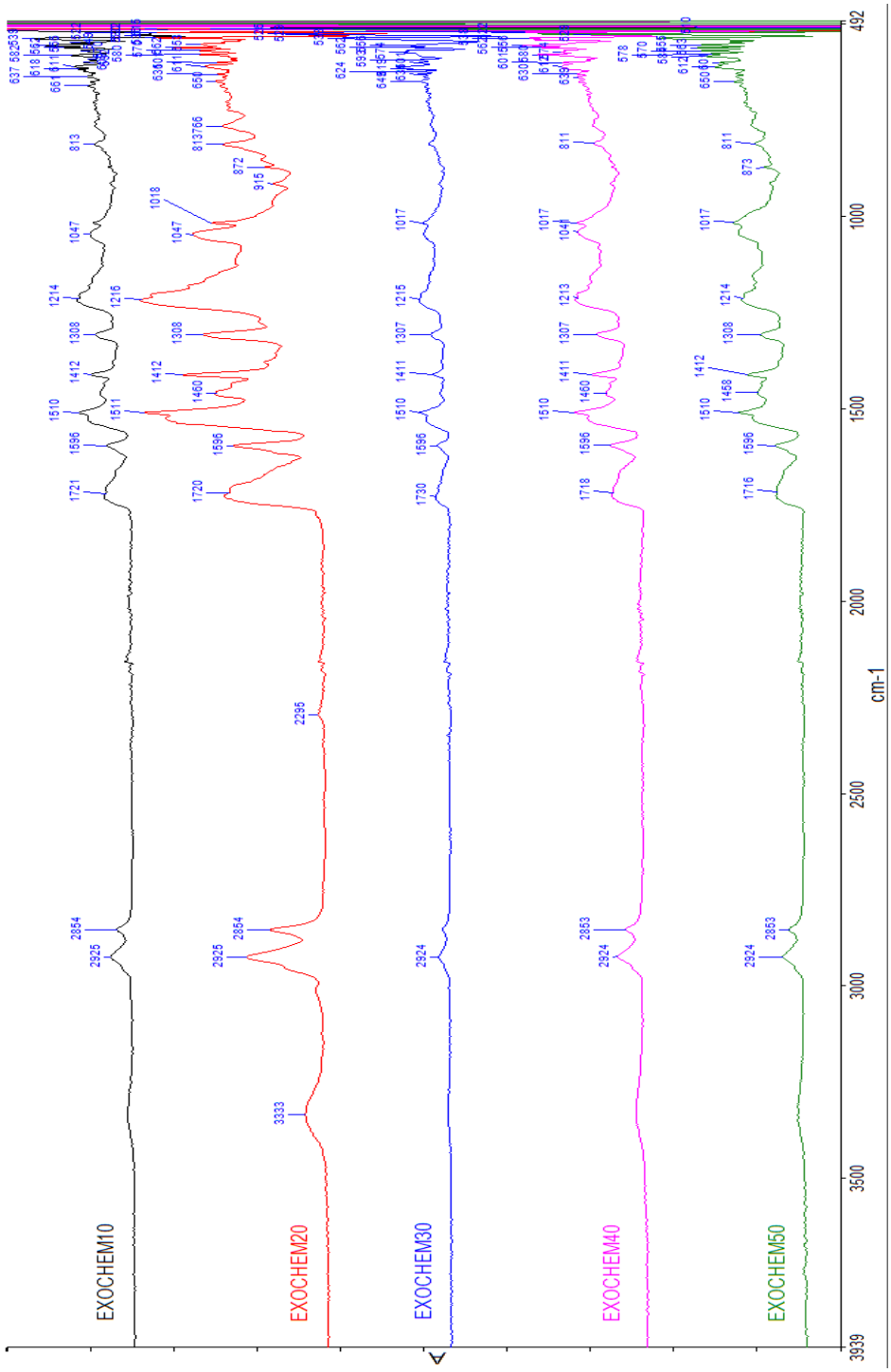

Figure 26-FTIR-ATR EXOCHEM samples

XI. Conclusion

Evidence from the above methods of characterization supports the initial aim of the study to investigate differences in gelatinized corn starch proportion and different foaming agents based on thermodynamic behavior in a blended foam material. From an overall perspective there are three main conclusions: first: foaming agent has an effect on mechanical and physical properties of the overall blend, second: the effect of gelatinized starch content is independent from foaming agent but still affects mechanical and physical properties of the blend and third: blends of gelatinized corn starch and pre-polymer made from castor oil and 4,4, methylene diphenyl diisocyanate were successfully prepared with viscoelastic and hydrophobic properties.

Findings that support the effect of foaming agent on foam blends are in cell structure measurements. The maximum cross sectional area for each foam blend occurs at different gelatinized corn starch proportions: ENDOPHY20, EXOCHEM30 and ENDOCHEM40, per plot 4. As for mechanical properties; modulus increases with cell cross sectional area for chemical foaming agents, in contrast modulus decreases with cross sectional area for a physical foaming agent, per plot 6.

Gelatinized corn starch proportion has an independent effect on physical properties of the blend as seen in figure16 and plot 2. In regards to plot 4 it is known that a maximum peak in cell cross sectional for ENDOCHEM samples occurs at 40(%w/w) gelatinized starch proportion but figure 16 shows ENDOCHEM40 to be comparatively the most dense, hence the effect if high M_w corn starch. Plot 2 provides evidence that density of foams increases with the increase in proportion of gelatinized starch most notably for ENDOPHY samples. Mechanical properties of foam samples suggest that gelatinized starch has greater influence than foaming agents based on plot 7, plots 11-13 and figure 22. Static cushion curves not only provided information on foam performance but also a practical understanding of compression properties measured. Such that plots 11-13 show a clear trend between samples differing in gelatinized starch content and shifts in deceleration values and static stress. On the other hand plots 8 -10 show the effect of foaming agents is unreliable. Plot 7 is very important because it indicates a response in the microstructure from the outside environment such that as samples exceed 20% gelatinized starch content effects of moisture are measureable due to additional free –OH- segments in gelatinized starch. Further support of gelatinized content on mechanical properties is seen in figure 22 where compression modulus at 68% stain shows the impact of increasing the hard segments in the overall blend.

As a final point, sample preparation was successful at creating hydrophobic samples based on results in plot 7 there is no effect of high humidity conditioning on all samples with 10 and 20 (% w/w) gelatinized starch. Once 20(%w/w) gelatinized starch content is exceeded a plasticizing effect of moisture is evident and logical. Viscoelastic nature of these samples is simply evident by the fact that cushion curves are able to be predicted. More supportive evidence is found within the FTIR spectra for all samples where urethane linkages with castor oil and gelatinized starch are detected.

Final comments on this should be made about the possibilities of future investigation. The shear rate of the blending procedure was observed to be low and perhaps not vigorous enough because the viscosity greatly increases during blending and overcame the torque of the mixing motor twice. These two factors together could produce interesting results. Another area of study would be validation of cushion performance and development of cushion factors (50). The fact that the foam is a blend could have unforeseen advantages over a homogenous foamed material. Furthermore there were some general observations made; over a period of months multiplied samples appeared to have growth of bacteria as seen by discoloration. Amds last; out of curiosity a 40 (%w/w) sample was left in a beaker of water and remained a float for a period of weeks.

Table 4 - Summary of Properties

Sample Name	Foaming Agent	OH mol	Density (g/cm³)	E Ambient (MPa)	E 90% R.H. (MPa)	Sensitivity (G's)	Area (mm²)	Count (#)
ENDOPHY10	none	0.51	0.30	5.86	5.73	14.81	1.76	25
ENDOPHY20	none	0.83	0.36	3.13	4.78	9.85	2.14	25
ENDOPHY30	none	1.23	0.37	21.34	13.92	13.00	1.77	25
ENDOPHY40	none	1.77	0.41	19.31	13.28	11.67	1.37	29
ENDOPHY50	none	2.52	0.46	15.90	26.61	13.29	0.86	37
ENDOCHEM10	**Sodium BiCarb., Citric acid, Stearic acid**	**0.54**	**0.27**	**7.84**	**6.91**	**11.13**	**0.30**	**45**
ENDOCHEM20	**Sodium BiCarb., Critic acid, Stearic acid**	**0.86**	**0.30**	**16.83**	**12.69**	**11.71**	**0.33**	**50**
ENDOCHEM30	**Sodium BiCarb., Citric acid, Stearic acid**	**1.26**	**0.32**	**11.36**	**7.73**	**11.85**	**0.29**	**35**
ENDOCHEM40	**Sodium BiCarb., Critic acid, Stearic acid**	**1.81**	**0.50**	**18.81**	**19.98**	**11.14**	**1.97**	**19**
ENDOCHEM50	**Sodium BiCarb., Citric acid, Stearic acid**	**2.57**	**0.52**	**16.04**	**18.18**	**11.25**	**0.91**	**32**
EXOCHEM10	Benzenesulfonly Hydrazide	0.51	0.25	6.42	6.28	12.76	0.23	39
EXOCHEM20	Benzenesulfonly Hydrazide	0.83	0.37	5.21	5.18	13.35	0.42	49
EXOCHEM30	Benzenesulfonly Hydrazide	1.23	0.36	18.62	11.34	10.39	2.05	24
EXOCHEM40	Benzenesulfonly Hydrazide	1.77	0.35	15.45	15.09	12.06	1.34	32
EXOCHEM50	Benzenesulfonly Hydrazide	2.52	0.56	20.04	31.51	11.06	0.53	34

XII. Appendices

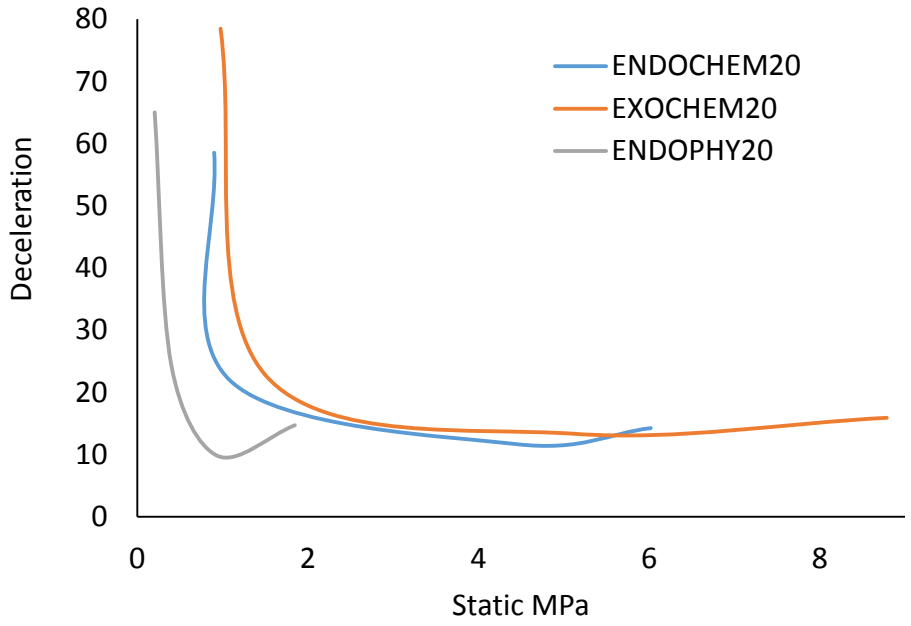

Plot 14- Static cushion curves for 20% (w/w) gelatinized starch samples

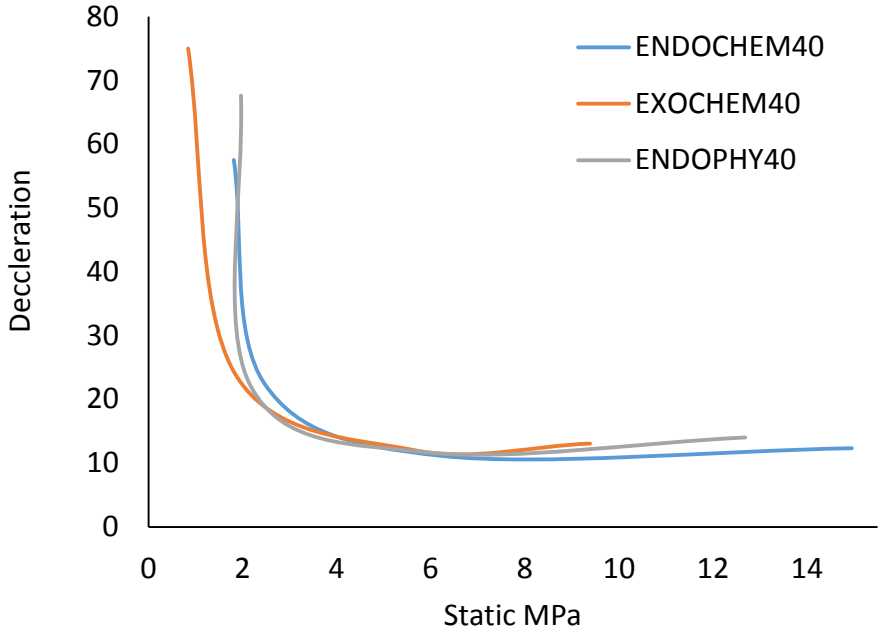

Plot 15- Static cushion curves for 40% (w/w) gelatinized starch samples

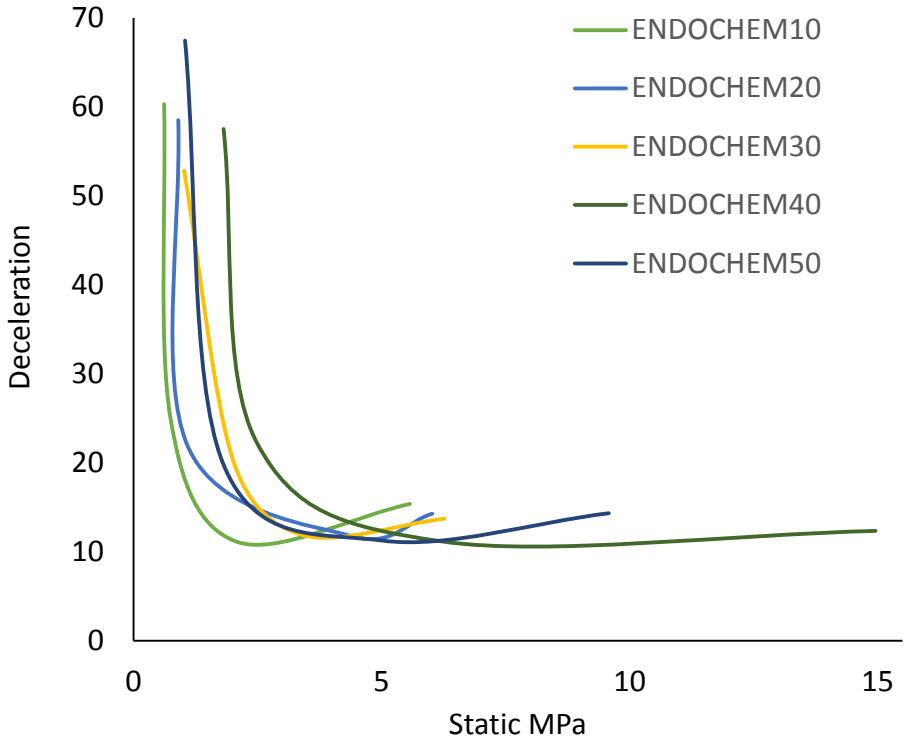

Plot 16-Static cushion curves for all ENDOCHEM samples

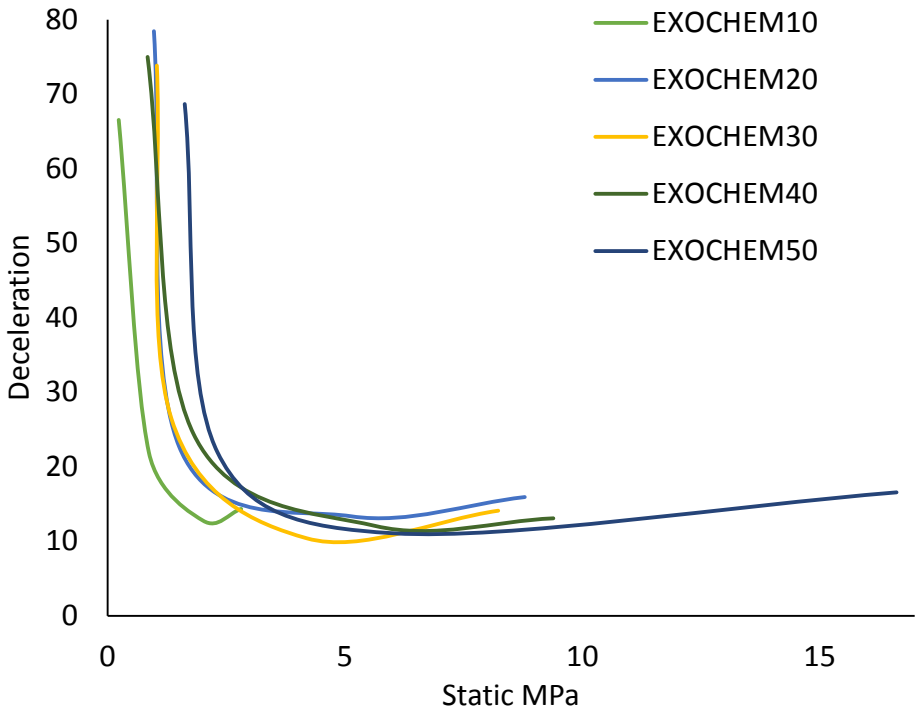

Plot 17-Static cushion curves for all EXOCHEM samples

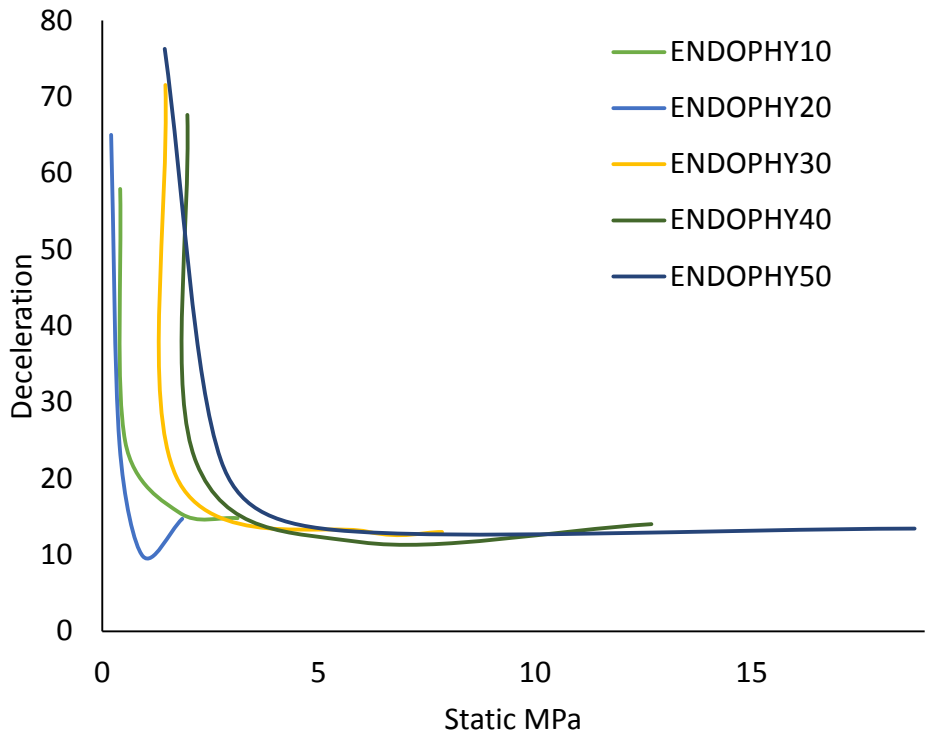

Plot 18-Static cushion curves for all ENDOPHY samples

Authors	Wave Number (cm-1)	Chain Segment	Behavior	Material
Gao, Z., Peng, J., Zhong, T., Sun, Jin., Wang, X. and Yue, C.	3600-3100	N-H	Stretching	PU
	1600-1760	C=0	Stretching	PU or CO
Wang, J, H., Rong, Z, M., Zhang, Q, M., Hu, J., Chen, W, H.,	3450	-OH- absop		CO
	1635	c=c		CO
Cao, X., Wang, Y. and Zhang, Y. (2005)	3300 (natural starch)	O-H	Stretching vibration	Starch
	2976	C-H	stretching	ethyl starch
	1727	C=O	Free	PU
	1708	C=O	hydrogen Bonded	PU
Wu, Q., Wu, Z., Tian, H., Zhang, Y. and Cai, S. (2008).	1643	C-H2	Bending	starch
	1744	C=O	stretching	CO
	1726	urethane groups	Free	PU
	1729 and 1512	urethane groups	Bonded to CO and Starch	PU
	1703-1744	urethane linakge		NCO2
	1704	hydrogen bonded urethane		PU H-BOND
Tan, L., Su, Q., Zhang, S. and Huang H. (2015)	3334	N-H	intramoleculer hydrogen bonds	PU
	1732	C=O	Free	PU
	1700	C=O	hydrogen Bonded	PU
	1645	O-H		CS or TPS
	2927	CH2	asymetric stretching	CS
Mosiewicki, A. M., Arciprete, A. G., Aranguren, I. M. and Marcovich, E. N. (2009).	722	C-H	*Cis* out of plane	CO
	2925, 2855,1463	C-H	stretch and bending	CO
	1164-1101	C-O	stretching	CO
Lu, Y., Tighzert, L., Dole, P. and Erre, D. (2005).	3388 and 3450	N-H	Stretching	PU H-BOND &
	1743 and 1720	C=O	Stretching	PU H-BOND &
	1529			

Table 5- Literature Review FTIR Spectrum

XIII. References

1. *Pereira, Helena, ed. Cork: Biology, Production and Uses. Amsterdam, NLD: Elsevier Science & Technology, 2007. ProQuest ebrary. Web. 16 June 2015.*

2. *Ecological Sustainability for Non-timber Forest Products. (2016). Google Books. Retrieved 21 June 2016, from https://books.google.com/books?id=ydgqBwAAQBAJ&pg=PT255&lpg=PT255&dq=2012+cork+producted&source=bl&ots=Nt_gbS66SM&sig=UU2RoGWc6jWxsxhCsKA9TEKLATI&hl=en&sa=X&ved=0CEkQ6AEwBmoVChMIsOC0uY-VxgIVi2OMCh1OQADS#v=onepage&q=2012%20cork%20producted&f=false*
3. *Dahl, R. (2010). Green Washing: Do You Know What You're Buying?Environmental Health Perspectives, 118(6), A246–A252.*
4. *Throne, J. L. (2004). Thermoplastic foam extrusion: An introduction. Cincinnati, Ohio; Munich, Germany: Hanser Publishers.*
5. *US plastic foams market. (2014,). PR Newswire*
6. *Painter, C. P. & Coleman, M. M. (1997). Fundamentals of Polymer Science: An Introductory Text 2nd Ed. Boca Raton, Florida: CRC Press LLC.*
7. *"British Plastics Federation." Moulding Expanded Polystyrene(EPS). N.p., n.d. Web 19June 2015.*
8. *A Guide to thermoplastic polyurethanes, Huntsman*
9. *Handbook of Polymer Foams. (2016).Google Books. Retrieved 21 June 2016, from https://books.google.com/books?id=TSFFFQSeKakC&pg=PP2&dq=Handbook+of+polymer+foams.+Shrewsbury,+United+Kingdom:+Rapra+Technology+Ltd.&hl=en&sa=X&ved=0ahUKEwjmm6LGr7nNAhWI0h4KHU-6Ap4Q6AEINjAA#v=onepage&q=Handbook%*
10. *(2016). Digitalcommons.calpoly.edu. Retrieved 21 June 2016, from http://digitalcommons.calpoly.edu/cgi/viewcontent.cgi?article=1043&context=it_fac*
11. *BASF, packaging with Styropor, PDF*

12. *Consulting, D. (2016). How It Works | Ecovative. Ecovativedesign.com. Retrieved 21 June 2016, from http://www.ecovativedesign.com/how-it-works*
13. *Green Cell Foam. (2016). Green Cell Foam. Retrieved 21 June 2016, from http://www.greencellfoam.com/green-cell-foam/*
14. *"Nonrenewable." EIA Energy Kids -. N.p., n.d. Web. 25 June 2015.*
15. *"National Forage & Grasslands Curriculum." Define the Terms Renewable Resource and Nonrenewable and Give Examples of Each Resource Type That Are Related to Forage Producti. N.p., n.d. Web. 25 June 2015.*
16. *"History of Polyurethanes." History of Polyurethanes. N.p., n.d. Web. 25 June 2015.*
17. *(2016). Icodassociates.com. Retrieved 14 June 2016, from http://www.icodassociates.com/docs/blowin*
18. *Blowing Agents and Foaming Processes 2013. (2013). Shrewsbury, GBR: Smithers Rapra. Retrieved from http://www.ebrary.com*

19. *Wittcoff, H. A., Reuben, B. G., & Plotkin, J. S. (2012). Industrial Organic Chemicals (3). Somerset, US: Wiley. Retrieved from http://www.ebrary.com9*
20. *Mutlu, H. and Meier, R. A. M. (2010). Castor Oil as a renewable resource for the chemical industry. European Journal of Lipid Science and Technology. DOI: 10.1002/ejlt.200900138*
21. *Ogunniyi, S. D. (2006). Castor Oil: A vital industrial raw material. Journal of Bioresource Technology. DOI: 10.1016/j.biortech.2005.03.028*
22. *Wang, S. and Copeland, L. (2013). Molecular disassembly of starch granules during gelatinization and its effect on starch digestibility: a review. Journal of Food and Function. DOI: 10.1039/c3fo60258c.*
23. *Zia, F., Zia, M. K., Zuber, M., Kamal, S. and Aslam, N. (2015) Starch based polyurethanes: A critical review updating recent literature. Journal of Carbohydrate Polymers. DOI: 10.1016/j.carbpol.2015.08.034*

24. *Shirke, A., Dholakiya, B. and Kuperkar, K. (2015). Novel Applications of Castor Oil Based Polyurethanes a Short Review. Journal of Polymer Science. DOI: 10.1134/S1560090415040132.*
25. *Dosmann, Lucian P., and Robert N. Steel. "Patent US3004934 - Flexible Shock-absorbing Polyurethane Foam Containing Starch and Method of preparing same." Google Books. N.p., 17 Oct. 1967. Web. 29 June 2015.*
26. *Bennett, Florence L., Felix M. Otey, and Charles L. Mehltretter. "Rigid Urethane Foam Extended with Starch. Http://cel.sagepub.com/content/3/8/369.full.pdf. Np.,n.d.Web*
27. *Otey, F. H., R. P. Westhoff, W. F. Kwolek, C. L. Mehltretter, and C. E. Rist. "Urethane Plastics Based on Starch and Starch-Derived Glycosides."Product R&D. N.p., n.d. Web. 02 July 2015*
28. *Otey, Felix H. "Current and Potential Uses of Starch Products in Plastics. " Http://naldc.nal.usda.gov/download/29667/pdf. N.p.,n.d. Web*
29. *F. H. Otey, R. P. Westhoff. and C. L. Mehltrette. "Reactivity of Modified starches with Isocyanates Retrieved from the journal of Starch Vol. 24, Issue 4, pages 107–110, 1972*
30. *Chen, Y., Zhang, L., Deng, R., and Liang, H. (2006) " Toughened Composites Prepared from Castor Oil Based Polyurthane and Soy Dreg by a One-Step Reactive Extrusion Process. Journal of Applied Polymer Science, Vol 101, p,953-960*
31. *Mistri, E., Routh, S., Ray, D., Sahoo, S., and Misra, M. (2011). Green composites from maleated castor oil and jute fibres. Journal of Industrial crops and Products. Vol 34 p. 900-906*
32. *Jute fibre | Wild Fibres natural fibres . (2016). Wildfibres.co.uk. Retrieved 21 June 2016, from http://www.wildfibres.co.uk/html/jute.html*
33. *Yildirim, N., Shaler, M. S., Gardner, J. D., Rice, R. and Bousfield,. W. D. (2014). Cellulose Nanofibril Reinforced Starch Insulating foams. Journal of Cellulose. DOI: 10.1007/s10570-014-0450-9.*
34. *Mosiewicki, A. M., Arciprete, A. G., Aranguren, I. M. and Marcovich, E. N. (2009). Polyurethane Foams Obtained from Castor Oil—based Polyol and Filled with Wood Flour. Journal of Composite Materials. DOI: 10.1177/0021998309345342.*

35. *Gao, Z., Peng, J., Zhong, T., Sun, Jin., Wang, X. and Yue, C. (2011) Biocompatible elastomer of waterborne polyurethane based on castor oil and polyethylene glycol with cellulose nanocrystals. Journal of Carbohydrate Polymers. DOI: 110.1016/j.carbpol.2011.10.027.*
36. *Lu, Y., Tighzert, L., Dole, P. and Erre, D. (2005). Preperation and properties of starch thermoplastics modified with waterborne polyurethane from renewable resources. Polymer Journal. DOI: 10.1016/j.polymer.2005.08.026*
37. *Kumar, M. and Kaur, R. (2013). Effect of Different formulations of MDI on Rigid Polyurethane Foams based on Castor Oil. International Journal of Scientific Research and Reviews. Vol 2. p. 29-42*
38. *Wang, J, H., Rong, Z, M., Zhang, Q, M., Hu, J., Chen, W, H., and Czigany, T. (2007). Biodegradable Foam plastics based on Castor Oil. Journal of Biomacromolecules. DOI: 10.1021/bm7009152.*
39. *Cao, X., Wang, Y. and Zhang, Y. (2005). Effects of Ethyl and Benzyl Groups on the Miscibility and properties of castor oil-based Polyurethane/Starch Derivative Semi-Interpenetrating Polymer Network. Journal of Macromolecule Bioscience. DOI: 10.1002/mabi.200500084.*
40. *Wu, Q., Wu, Z., Tian, H., Zhang, Y. and Cai, S. (2008). Structure and Properties of Tough Thermoplastic Starch Modified with Polyurethane Micro particles. Journal of Industrial & Engineering Chemistry Research. DOI: 10.1021/ie801005w.*
41. *SpillTech.(2016). Chemical Compatibility Guide For Polyurethane Items. Technical Data sheet.*
42. *Skočilas, J., Žitný, R and Šesták, J. (2010). Starch Foam Expansion in Closed Mold. Journal of Food Bioprocess Technology. DOI: 10.1007/s11947-010-0348-y.*
43. *Tan, L., Su, Q., Zhang, S. and Huang H. (2015). Preparing thermoplastic polyurethane/thermoplastic starch with high mechanical and biodegradable properties. The Journal of the Royal Society of Chemistry. DOI: 10.1039/c5ra09713d.*
44. *Valero, F, M., Pulido, E, J., Hernandez, C, J., Posada, A, J. and Ramirez, A. (2009). Preparation and Properties of Polyurethanes based on Castor Oil Chemically Modified*

with Yucca Starch Glycoside. Journal of Elastomers and Plastics. DOI: 10.1177/0095244308091785.

45. *Xiong, Z., Zhang, L., Ma, S., Yang, Y., Zhang, C., Tang, Z. And Zhu, J. (2013). Effect of castor oil enrichment layer produced by reaction on the properties of PLA/HDI-g-starch blends. Journal of Carbohydrate Polymers. DOI: 10.1016/j.carbpol.2013.01.038*
46. *Wang, C., Zheng, Y., Xie, Y., Qiao, K., Sun, Y. and Yue, L. (2015). Synthesis of bio-castor oil polyurethane flexible foams and the influence of biotic component on their performance. Journal of Polymer Research. DOI: 10.1007/s10965-015-0782-7*
47. *Sharma, F., Kumar, S., Unni, R. A., Vinod, K. A., Rath, K. S. and Harikrishnan, G. (2014). Foam stability and polymer Phase Morphology of Flexible Polyurethane Foams Synthesized from Castor Oil. Journal of Applied Polymer Science. DOI: 10.1002/app.40668.*
48. *Kim, D., Kwon, O., Yang, S., Park, J., & Chun, B. (2007). Structural, thermal, and mechanical properties of polyurethane foams prepared with starch as the main component of polyols. Fibers Polym, 8(2), 155-162. doi:10.1007/bf02875785*
49. *Goods, H. S., Neuschwanger, L. C., Henderson, C. and Skala, M. D.(1997). Mechanical Properties and Energy Absorption Characteristics of a Polyurethane Foam. Prepared by Sandia National Laboratories. Retrieved form: http://www.osti.gov/scitech/servlets/purl/485941/*
50. *Ge, C., and Huang, H. (2014). Corner foam versus Flat Foam: An Experimental Comparison on Cushion Performance. Journal of Packaging Technology and Science. DOI: 10.1002/pts.2098*
51. *Courtesy of Csp.umn.edu. Retrieved 27 June 2016, from http://csp.umn.edu/wp-content/uploads/2015/03/Starch-to-Plastics-Lab-March_26_2015.pdf*
52. *Rieger, B., Künkel, A., Coates, W. G. et al. (2011). Synthetic Biodegradeable Polymers. Advances in Polymer Science. DOI 10.1007/978-3-642-27154-0*
53. *Sodium bicarbonate. (2016).Webbook.nist.gov. Retrieved 10 August 2016, from http://webbook.nist.gov/cgi/formula?ID=B6007910&Mask=80*